



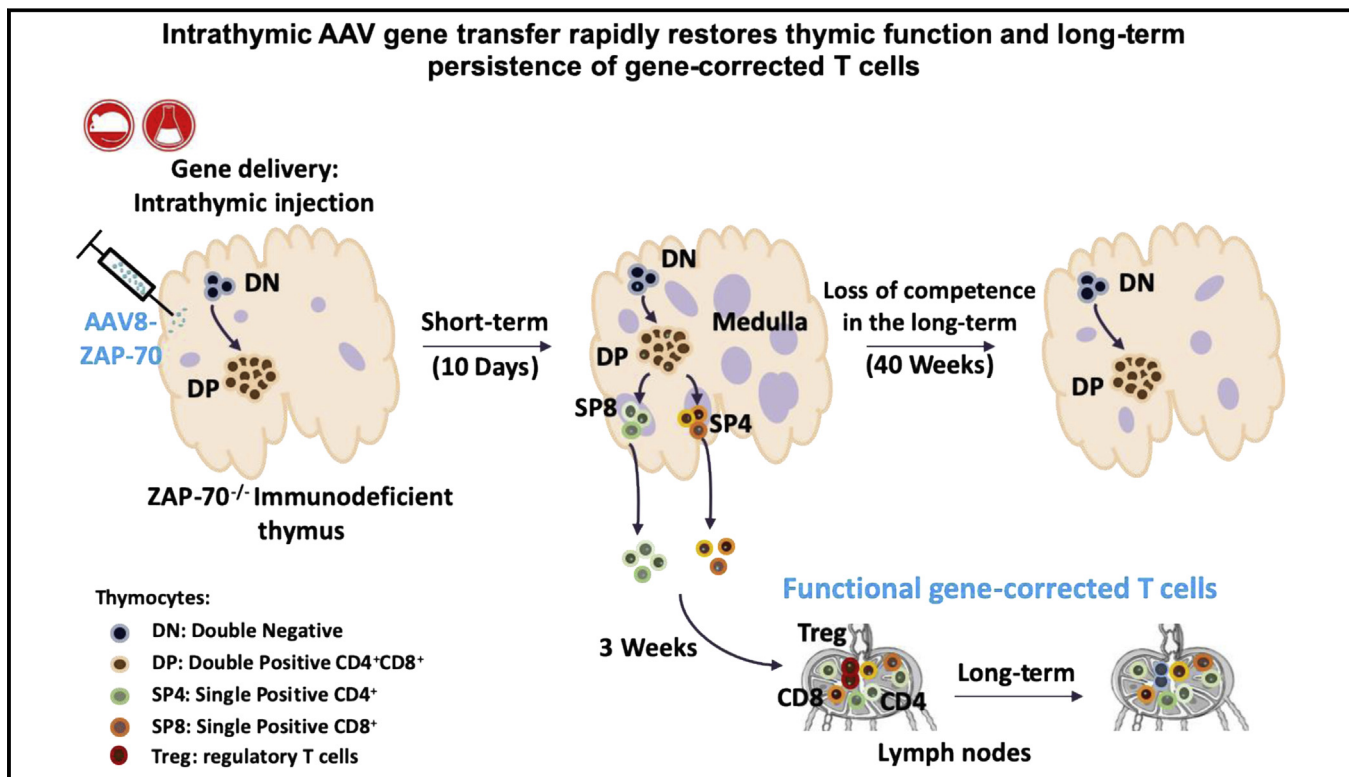
# Intrathymic adeno-associated virus gene transfer rapidly restores thymic function and long-term persistence of gene-corrected T cells

Marie Pouzolles, PhD,<sup>a</sup> Alice Machado, MSc,<sup>a,\*</sup> Mickaël Guilbaud, MSc,<sup>b,\*</sup> Magali Irla, PhD,<sup>c</sup> Sarah Gailhac, MSc,<sup>a</sup> Pierre Barennes, MSc,<sup>d</sup> Daniela Cesana, PhD,<sup>e</sup> Andrea Calabria, PhD,<sup>e</sup> Fabrizio Benedicenti, PhD,<sup>e</sup> Arnauld Ségué, PhD,<sup>f</sup> Indu Raman, MSc,<sup>g</sup> Quan-Zhen Li, MD, PhD,<sup>g,h</sup> Eugenio Montini, PhD,<sup>e</sup> David Klatzmann, MD, PhD,<sup>d,i</sup> Oumeya Adjali, MD, PhD,<sup>b</sup>

Naomi Taylor, MD, PhD,<sup>a,j</sup> and Valérie S. Zimmermann, PhD<sup>a</sup>

Montpellier, Nantes, Marseille, and Paris, France; Milan, Italy; Dallas, Tex; and Bethesda, Md

## GRAPHICAL ABSTRACT



From <sup>a</sup>Institut de Génétique Moléculaire de Montpellier, University of Montpellier, CNRS, Montpellier; <sup>b</sup>INSERM UMR1089, Université de Nantes, Centre Hospitalier Universitaire de Nantes; <sup>c</sup>the Center of Immunology Marseille-Luminy (CIML), INSERM U1104, CNRS UMR7280, Aix-Marseille Université UM2, Marseille; <sup>d</sup>Sorbonne Université, INSERM, Immunology-Immunopathology-Immunotherapy (i3), Paris; <sup>e</sup>the San Raffaele Telethon Institute for Gene Therapy (SR-Tiget), IRCCS, San Raffaele Scientific Institute, Milan; <sup>f</sup>Aix Marseille University, CNRS, INSERM, Institut Paoli-Calmettes, CCRM, Marseille; <sup>g</sup>the Microarray Core Facility, University of Texas Southwestern Medical Center, Dallas; <sup>h</sup>the Department of Immunology, University of Texas Southwestern Medical Center, Dallas; <sup>i</sup>AP-HP, Hôpital Pitié-Salpêtrière, Biotherapy (CIC-BTi) and Inflammation-Immunopathology-Biotherapy Department (i2B), Paris; and <sup>j</sup>Pediatric Oncology Branch, Center for Cancer Research, National Cancer Institute, National Institutes of Health, Bethesda.

\*These authors contributed equally to this work.

M.P. was supported by a PhD fellowship from the LABEX EpiGenMed and the FRM. M.I. and O.A. are supported by INSERM. N.T. was supported by INSERM and the National Institutes of Health, and V.S.Z. is supported by CNRS. This work was funded by

the AFM, grant R01AI059349 from the National Institute of Allergy and Infectious Diseases, and the ANR, ARC, FRM, INCA, and ERC-Advanced TRIPoD (#322856 to D.K.).

Disclosure of potential conflict of interest: The authors declare that they have no relevant conflicts of interest.

Received for publication November 6, 2018; revised July 28, 2019; accepted for publication August 5, 2019.

Available online September 9, 2019.

Corresponding author: Oumeya Adjali, MD, PhD, Naomi Taylor, MD, PhD, or Valérie S. Zimmermann, PhD, Institut de Génétique Moléculaire de Montpellier, 1919 Route de Mende, 34293 Montpellier, Cedex 5, France. E-mail: oumeya.adjali@univ-nantes.fr. Or: taylorn4@mail.nih.gov. Or: zimmermann@igmm.cnrs.fr.

The CrossMark symbol notifies online readers when updates have been made to the article such as errata or minor corrections

0091-6749/\$36.00

© 2019 American Academy of Allergy, Asthma & Immunology  
<https://doi.org/10.1016/j.jaci.2019.08.029>

**Background:** Patients with T-cell immunodeficiencies are generally treated with allogeneic hematopoietic stem cell transplantation, but alternatives are needed for patients without matched donors. An innovative intrathymic gene therapy approach that directly targets the thymus might improve outcomes.

**Objective:** We sought to determine the efficacy of intrathymic adeno-associated virus (AAV) serotypes to transduce thymocyte subsets and correct the T-cell immunodeficiency in a zeta-associated protein of 70 kDa (ZAP-70)-deficient murine model.

**Methods:** AAV serotypes were injected intrathymically into wild-type mice, and gene transfer efficiency was monitored. ZAP-70<sup>-/-</sup> mice were intrathymically injected with an AAV8 vector harboring the ZAP70 gene. Thymus structure, immunophenotyping, T-cell receptor clonotypes, T-cell function, immune responses to transgenes and autoantibodies, vector copy number, and integration were evaluated.

**Results:** AAV8, AAV9, and AAV10 serotypes all transduced thymocyte subsets after *in situ* gene transfer, with transduction of up to 5% of cells. Intrathymic injection of an AAV8-ZAP-70 vector into ZAP-70<sup>-/-</sup> mice resulted in a rapid thymocyte differentiation associated with the development of a thymic medulla. Strikingly, medullary thymic epithelial cells expressing the autoimmune regulator were detected within 10 days of gene transfer, correlating with the presence of functional effector and regulatory T-cell subsets with diverse T-cell receptor clonotypes in the periphery. Although thymocyte reconstitution was transient, gene-corrected peripheral T cells harboring approximately 1 AAV genome per cell persisted for more than 40 weeks, and AAV vector integration was detected.

**Conclusions:** Intrathymic AAV-transduced progenitors promote a rapid restoration of the thymic architecture, with a single wave of thymopoiesis generating long-term peripheral T-cell function. (J Allergy Clin Immunol 2020;145:679-97.)

**Key words:** Severe combined immunodeficiency, gene therapy, zeta-associated protein of 70kDa, thymus, intrathymic gene transfer, medulla formation, T-cell reconstitution, humoral immunity

Primary immunodeficiency diseases consist of a heterogeneous group of more than 200 genetic disorders,<sup>1</sup> with severe combined immunodeficiency (SCID) characterized by defective T- and B-lymphocyte function. Transplantation of histocompatible hematopoietic stem cells (HSCs) is the optimal treatment for infants with SCID, but in the absence of histocompatible donors, these patients typically receive an HSC transplant from HLA-haploidentical donors. In the latter case T cells are extensively depleted from the graft in an effort to prevent graft-versus-host disease. Although recent modifications of this protocol have resulted in an increased survival rate, significant short-term and long-term complications are still reported, and the lag time during which the patient remains susceptible to infections is quite long.<sup>2</sup> Thus, although this treatment is generally successful, it remains important to develop new therapeutic approaches.

Significant efforts have gone into developing gene therapy strategies for these patients. Indeed, gene therapy trials for X-linked SCID and, more recently, for adenosine deaminase deficiency and Wiskott-Aldrich syndrome demonstrated that this strategy can cure human disease, and they have continued to marketing approval.<sup>3-12</sup> The selective advantage of corrected progenitors and the massive expansion of corrected T cells has

#### Abbreviations used

AAV:	Adeno-associated virus
AIRE:	Autoimmune regulator
BGH:	Bovine growth hormone
CTLA4:	Cytotoxic T lymphocyte-associated antigen 4
DN:	CD4 <sup>-</sup> CD8 <sup>-</sup> double negative
DP:	CD4 <sup>+</sup> CD8 <sup>+</sup> double positive
dsDNA:	Double-stranded DNA
FOXP3:	Forkhead box P3
GFP:	Green fluorescent protein
GITR:	Glucocorticoid-induced TNFR family related gene
Hprt:	Hypoxanthine phosphoribosyltransferase
HSC:	Hematopoietic stem cell
KO:	Knockout
LC:	Linker cassette
mTEC:	Medullary thymic epithelial cell
OVA:	Ovalbumin
qPCR:	Quantitative PCR
rAAV:	Recombinant adeno-associated virus
RNP:	Ribonucleoprotein
scAAV:	Self-complementary adeno-associated virus
SCID:	Severe combined immunodeficiency
SP4:	Single-positive CD4
SP8:	Single-positive CD8
SSA:	Sjögren syndrome-related antigen A
TCR:	T-cell receptor
TEC:	Thymic epithelial cell
Treg:	Regulatory T
WT:	Wild-type
ZAP-70:	Zeta-associated protein of 70kDa

facilitated this success. Adverse events caused by insertional mutagenesis of gammaretroviral vectors<sup>13-16</sup> have resulted in the development of lentivirus-based clinical trials for patients with SCID. Notably, mutagenesis has not been reported in the latter,<sup>5,17,18</sup> but it is still important to continue to explore and develop new therapeutic strategies.

After transplantation of patients with SCID with allogeneic healthy HSCs or gene-corrected autologous HSCs, T-lymphocyte differentiation occurs in the thymus.<sup>19</sup> These HSCs, administered by means of intravenous injection, must continuously home to the thymus because under physiologic conditions, thymic settling progenitors are only able to give rise to a single round of thymocyte differentiation.<sup>20-23</sup> Notably, however, intrathymic injection of HSCs, as well as pro-T cells, improves T-cell differentiation in the thymus<sup>24-31</sup> and increases the expansion of supporting thymic epithelial cells (TECs).<sup>32</sup> Additionally, the thymus can be targeted through direct injection of antigens or vectors expressing genes of interest,<sup>33-37</sup> with recombinant adeno-associated virus (rAAV) vectors transducing thymocytes with a 10-fold greater efficiency than lentiviral vectors.<sup>34,37</sup> Indeed, rAAV vectors hold great promise for gene transfer therapies because they are capable of infecting nondividing cells, and particles of high titer and purity can be produced.<sup>38-42</sup>

rAAV vectors were initially developed as single-stranded viral DNA vectors. The transduction efficiency of these “conventional” rAAV vectors based on the AAV2 serotype is known to be tissue-dependent, with significant gene transfer in various tissues<sup>43-48</sup> but only low-level infection of murine hematopoietic

cells.<sup>49-51</sup> However, several AAV serotypes have exhibited increased ability to transduce HSCs,<sup>40,52-56</sup> and long-term transgene persistence has been detected.<sup>54,55,57</sup>

In an attempt to achieve efficient gene transfer in the thymus and correct T-cell deficiency, we evaluated *in situ* intrathymic gene transfer using rAAV2 vectors cross-packaged into AAV8, AAV9, and AAV10 serotypes. Intrathymic administration of all 3 serotypes led to transgene expression in all thymocyte subsets, but AAV8 exhibited the greatest gene transfer efficiency, resulting in transduction of up to 5% of all thymocytes. Using mice that are immunodeficient because of mutations in the zeta-associated protein of 70 kDa (ZAP-70) protein tyrosine kinase<sup>58</sup> as a paradigm, we found that intrathymic injection of an AAV2/AAV8-ZAP-70 vector resulted in the development of gene-corrected mature thymocytes within 10 days of gene transfer. Concurrently, AAV8-ZAP-70 gene transfer promoted development of the thymic medulla, containing autoimmune regulator (AIRE)-expressing medullary thymic epithelial cells (mTECs), which mediate T-cell tolerance. Furthermore, AAV-transduced T cells were detected in the peripheral circulation by 2 weeks, and these T cells exhibited long-term function for greater than 10 months, responding robustly to T-cell receptor (TCR) stimulation. Thus the thymus immune niche can be shaped by an intrathymic AAV-based strategy, accelerating restoration of its architecture and facilitating a transient thymocyte differentiation with long-term peripheral T-cell function.

## METHODS

AAV vector stocks harboring the green fluorescent protein (*GFP*) or ZAP70 genes were administered by means of intrathymic injection into wild-type (WT) C57Bl/6 and ZAP-70<sup>-/-</sup> mice, as indicated. All animal experiments were performed in accordance with the recommendations of the CNRS Animal Care Committee and were consistent with the guidelines set by the Panel on Euthanasia and the National Institutes of Health “Guide for the care and use of laboratory animals.” T-cell reconstitution was monitored by using flow cytometry, and frozen thymic sections were stained, as previously described.<sup>59</sup> Vector genomes were monitored by using real-time PCR. For integration analyses, we adopted a sonication-based linker-mediated PCR method, as previously described.<sup>60,61</sup> Anti-ovalbumin (OVA) IgG responses were evaluated after OVA immunization; serum anti-ZAP-70 antibodies, as well as anti-double-stranded DNA (dsDNA), anti-ribonucleoprotein (RNP), and anti-Sjögren syndrome-related antigen A (SSA) antibodies, were evaluated by using an ELISA; neutralizing antibodies were monitored, as previously described<sup>62</sup>; and gene expression (forkhead box P3 [*Foxp3*] and *Il10*) was evaluated by using quantitative RT-PCR. The TCR repertoire was evaluated by means of deep sequencing, and data were analyzed with R Studio software. Screening for IgM/IgG reactivity against autoantigens was performed by using autoantibody arrays.<sup>63,64</sup> The detailed methods are available in this article’s Online Repository at [www.jacionline.org](http://www.jacionline.org).

## RESULTS

### Intrathymic AAV8 gene therapy reconstitutes the thymus architecture within 1.5 weeks and promotes transient thymocyte differentiation

We first assessed the potential of self-complementary rAAV2 vectors harboring the *GFP* transgene and pseudotyped with the 8-, 9-, and 10-capsid serotypes to transduce the murine thymus. Our analyses revealed thymocyte transduction by all 3 serotypes; efficiencies in nonconditioned immunocompetent mice ranged from 2% to 5% by 3 days after injection (Fig 1, A). Transduced cells were found in all subsets, including the most immature

CD4<sup>-</sup>CD8<sup>-</sup> double-negative (DN) and CD4<sup>+</sup>CD8<sup>+</sup> double-positive (DP) and the most mature single-positive CD4 (SP4) and single-positive CD8 (SP8) thymocytes (Fig 1, A and B). Mice transduced with AAV9 vectors exhibited lower levels of DP thymocytes within both the nontransduced and transduced subsets, suggesting a possible toxicity (Fig 1, A and B).

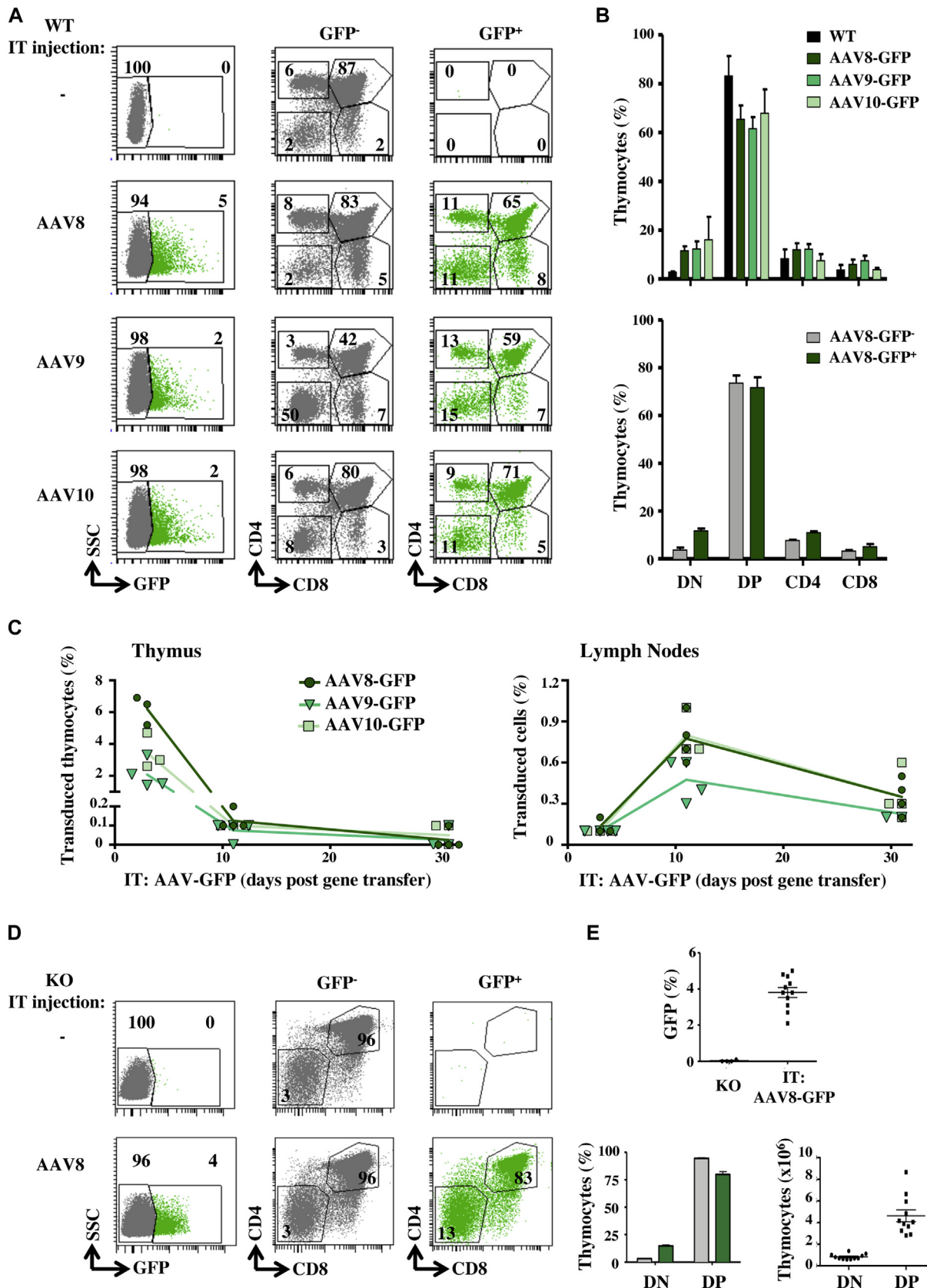
However, total thymocyte numbers were not significantly altered, with a mean of  $180 \times 10^6$  thymocytes per thymus. Furthermore, in mice undergoing intrathymic administration with the AAV2/AAV8 vector, repartition of thymocyte subsets remained stable (Fig 1, B).

After thymocyte transduction, mature SP4 and SP8 thymocytes migrated to the periphery, strikingly representing up to 1% of peripheral T lymphocytes in lymphoid-replete WT mice at day 10 (Fig 1, C). However, gene-transduced peripheral T cells decreased by 2-fold at day 30, likely because of the emigration of newly differentiated mature thymocytes. Given the high-level transduction of thymocytes by AAV8, including immature DN thymocyte progenitors, we studied the potential of this serotype to correct thymocyte differentiation in an immunodeficient mouse model.

Using a model of ZAP-70-deficient mice, exhibiting an arrest in thymocyte differentiation at the DP stage,<sup>58</sup> we assessed whether intrathymic administration of an AAV8 vector could be used to efficiently achieve gene transfer in defective thymocytes. Importantly, 3 days after intrathymic transfer of the AAV2/AAV8-GFP vector used above (Fig 1, A), transduction of both DN and DP thymocytes was detected (Fig 1, D). Notably, gene transfer was detected in 2% to 5% of ZAP-70<sup>-/-</sup> thymocytes, resulting in transduction of a mean of  $0.8 \times 10^6$  DN thymocytes and  $4.6 \times 10^6$  DP thymocytes ( $n = 11$ ; Fig 1, D). Thus the level of intrathymic AAV8 transduction in thymocytes of ZAP-70<sup>-/-</sup> immunodeficient mice was similar to that detected in WT mice, supporting use of this strategy for gene transfer.

Defects in the development of SP thymocytes, irrespective of the mutation, result in lack of a functional thymic medulla, and it is likely that these stromal abnormalities contribute to immune dysregulation in the thymus.<sup>65,66</sup> Defective medulla formation is classically associated with a lack of mTECs expressing AIRE. Its absence results in aberrant T-cell selection<sup>67</sup> and subsequent development of autoreactive T cells.<sup>68,69</sup> Using a transgenic model, it has been shown that the leaky differentiation of as few as  $3.5 \times 10^5$  nontransgenic SP4 thymocytes bearing TCRs with reactivities against self-antigens is sufficient for formation of a functional medulla.<sup>70</sup> Because we detected transduction of more than  $1 \times 10^6$  DN/DP thymocytes in ZAP-70<sup>-/-</sup> mice using an AAV8 gene transfer approach (Fig 1, E), we hypothesized that an intrathymic AAV8 gene therapy strategy might promote generation of sufficient SP4 thymocytes for medulla formation.

Therefore we assessed whether thymic architecture is modified by the intrathymic administration of single-stranded AAV8-ZAP-70 virions ( $1.3 \times 10^{13}$  vector genomes/kg). In the absence of gene transfer, thymi of ZAP-70<sup>-/-</sup> mice harbored only a minimal medulla, with a mean of  $115 \text{ AIRE}^+ \text{ cells/mm}^2$  of tissue (Fig 2, A and B). Notably, within 10 days after intrathymic AAV8-ZAP-70 gene transfer, there was a dramatic generation of medullary tissue, and the number of AIRE<sup>+</sup> mTECs increased significantly to  $295 \text{ AIRE}^+ \text{ cells/mm}^2$  of tissue ( $P < .001$ ; Fig 2, A and B). Although numbers of AIRE<sup>+</sup> cells decreased between 3 and 10 weeks after intrathymic AAV8-ZAP-70 gene transfer ( $154 \text{ AIRE}^+ \text{ cells/mm}^2$  to  $95 \text{ AIRE}^+ \text{ cells/mm}^2$ ), they remained



significantly greater than those in age-matched ZAP-70<sup>-/-</sup> mice treated with control AAV8-GFP vector ( $P < .05$ ; Fig 2, B). Moreover, medulla development was robust, increasing from less than 0.03 mm<sup>2</sup> to 0.06 mm<sup>2</sup> by 1.5 weeks after gene transfer ( $P < .01$ ; see Fig E1, A, in this article's Online Repository at [www.jacionline.org](http://www.jacionline.org)). It is interesting to note that the medullary area remained significantly increased for the first 3 weeks after gene transfer but then decreased at week 10, suggesting transient thymic reconstitution (see Fig E1, A).

Because medulla formation and generation of AIRE<sup>+</sup> mTECs are dependent on cross-talk with mature SP thymocytes,<sup>65,66,68,69</sup> these data strongly suggest that T-cell differentiation proceeds rapidly after intrathymic gene delivery. Furthermore, mTEC turnover is estimated at 2 to 3 weeks,<sup>71,72</sup> suggesting that the decrease in AIRE<sup>+</sup> cell numbers that we observed at 10 weeks after gene transfer (Fig 2, B) was associated with a single wave of thymocyte differentiation. Indeed, within the WT thymus, percentages of gene-transduced cells that represented mature SP4 and SP8 thymocytes peaked at day 10 after gene transfer, likely representing maturation of DP thymocytes,<sup>27,73,74</sup> and decreased by 3 weeks, which is consistent with SP thymocyte emigration ( $P < .01$ ; Figs 1, C, and 2, C).<sup>75</sup> Differentiation of SP4 and SP8 thymocytes was detected in AAV8-ZAP-70-treated ZAP-70<sup>-/-</sup> mice but was not associated with a significant change in total thymocyte numbers, likely because of similar initial thymocyte numbers in the WT and knockout (KO) mice (see Fig E1, B). Notably, maturation of gene-transduced SP8 thymocytes in intrathymic AAV8-ZAP-70–corrected ZAP-70<sup>-/-</sup> mice followed a kinetics similar to that detected in WT mice (Fig 2, C). SP4 thymocytes peaked even earlier at 3 days after transduction (Fig 2, C, right panel;  $P < .01$ ). These data are in agreement with the kinetic signaling model of thymocyte differentiation in which all DP thymocytes are first signaled to an intermediate SP4 thymocyte fate before SP8 differentiation.<sup>76</sup>

Mature SP thymocytes were detected at all time points in WT mice, but as expected from the physiologic involution of the thymus with age, absolute numbers of SP thymocytes decreased between 0.5 (3 days) and 3 weeks after gene transfer (note that mice were 3 weeks of age at the time of gene transfer; Fig 2, D). Total numbers of SP thymocytes in ZAP-70<sup>-/-</sup> mice after AAV8-ZAP-70 gene transfer were greater than  $2 \times 10^6$  at 3 days after gene transfer (Fig 2, D). Consistent with the gradual loss of AIRE<sup>+</sup> cells and the decreasing medulla size after intrathymic gene correction (Fig 2, B), SP thymocytes decreased to baseline levels at 3 weeks (Fig 2, D). Together, these data strongly suggest that intrathymic AAV gene correction provides for a single wave of thymocyte differentiation.

## Intrathymic AAV8-ZAP-70 transduction promotes long-term maintenance of peripheral T cells and T lineage-specific gene transfer

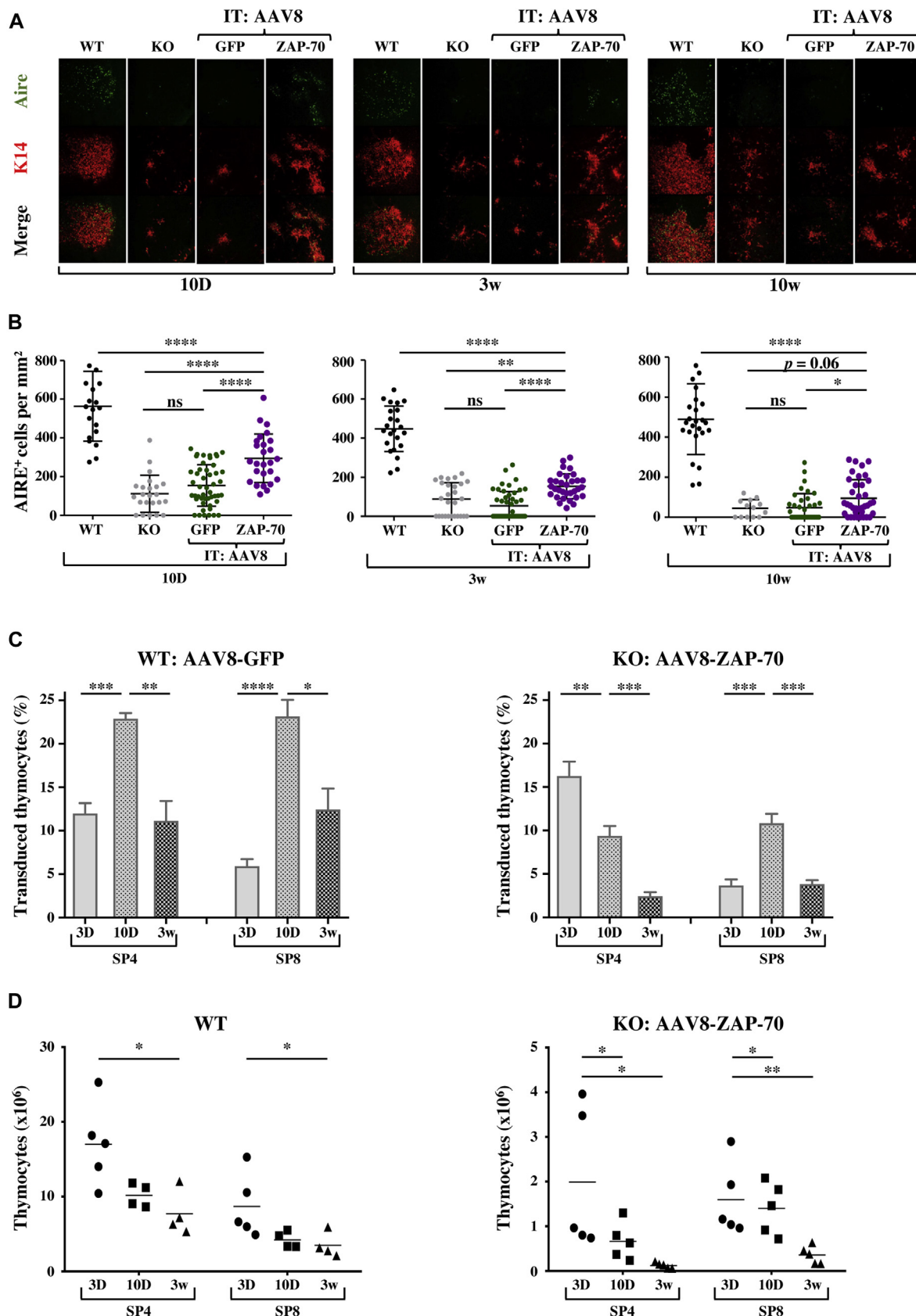
Consistent with the kinetics of thymocyte differentiation and emigration,<sup>27,73,75,77</sup> gene-corrected T cells were detected in the bloodstream within 3 weeks after intrathymic transfer (Fig 3, A). T cells were monitored in peripheral blood samples between 3 and 40 weeks after transduction. It is notable that a single wave of T-cell differentiation allowed for maintenance of a stable level of peripheral T cells for the 40-week evaluation period (>10 months). AAV8-ZAP-70–transduced KO mice exhibited a significantly greater percentage of peripheral T cells relative to KO or intrathymic AAV8-ZAP-70–transduced KO mice at all time points evaluated: 3 to 10 weeks, 11 to 20 weeks, 21 to 30 weeks, and 31 to 40 weeks ( $P < .0001$  for all time points; Fig 3, A).

The thymus is the site of T-cell differentiation, but B cells and hematopoietic progenitors with myeloid lineage potential are also present in this organ.<sup>78,79</sup> Furthermore, AAV virions can diffuse, potentially resulting in transduction of other cell types.<sup>80,81</sup> Therefore it was important to compare transduction of T cells and non-T cells by AAV8-ZAP-70 virions after intrathymic gene transfer. As expected, almost 100% of all peripheral T cells, encompassing both CD4 and CD8 subsets, expressed the AAV8-encoded ZAP-70 transgene (Fig 3, B). Notably, however, transgene expression was not detected in significant levels in non-T-cell hematopoietic lineages, including B cells and myeloid cells, or in the bone marrow during the entire 40-week follow-up period (Fig 3, B). Furthermore, expression levels of ectopic ZAP-70 in gene-transduced peripheral T cells were approximately 2- to 4-fold greater than endogenous levels monitored as a function of mean fluorescence intensity, and these levels did not significantly change during the 40-week follow-up (Fig 3, C).

We next assessed whether maintenance of transduced T cells in the peripheral circulation was associated with a stable percentage and number of CD3<sup>+</sup> T cells in the lymph nodes of AAV8-ZAP-70–treated mice (Fig 3, D). Although T-cell levels were significantly lower than those detected in WT mice, both in percentages and absolute numbers, they were induced by 3 weeks after intrathymic transduction, revealing the rapid initial wave of AAV transgene–mediated thymocyte differentiation. Furthermore, they remained stable for more than 10 months. Progression of immature DP thymocytes through positive selection requires ZAP-70–dependent TCR signaling.<sup>82,83</sup>

Positively selected DP thymocytes then undergo CD4/CD8 lineage choice, a complex process that has been shown to occur through kinetic signaling. Under conditions of persistent TCR signaling, CD4 T-cell differentiation occurs, whereas MHC class

**FIG 1.** AAV8, AAV9, and AAV10 serotypes efficiently transduce all thymocyte subsets. **A**, scAAV8, scAAV9, and scAAV10 serotypes harboring GFP were administered intrathymically into WT mice, and GFP expression was assessed at day 3. Representative CD4/CD8 profiles from nontransduced (gray) and transduced (green) GFP<sup>+</sup> thymocytes are presented. **B**, Quantification of percentages of GFP<sup>+</sup> DN, DP, SP4, and SP8 thymocytes are shown and compared with those in nontransduced WT mice (upper panel). Thymocyte subset repartition within nontransduced (GFP<sup>-</sup>) and transduced (GFP<sup>+</sup>) compartments of AAV8-GFP–transduced mice are presented (lower panel; means  $\pm$  SEMs). **C**, Percentages of GFP<sup>+</sup> thymocytes and lymph node T cells are presented as a function of time ( $n = 3-5$  mice per time point). **D**, Representative plots of GFP<sup>-</sup> and GFP<sup>+</sup> thymocytes at day 3 after intrathymic injection of the scAAV-GFP vector into ZAP-70<sup>-/-</sup> (KO) mice (left). Quantification of GFP<sup>+</sup> cells in KO and AAV-transduced KO mice ( $n = 11$ ) are presented (top). Mean percentages of DN and DP thymocytes within the nontransduced (GFP<sup>-</sup>, gray) and transduced (GFP<sup>+</sup>, green) subsets (left bottom panel), as well as absolute numbers of transduced GFP<sup>+</sup> thymocytes, are shown (right bottom panel). IT, Intrathymic; SSC, side scatter.



I-specific CD8 T cells only differentiate after a disruption of MHC class II/TCR signals and subsequent cytokine signaling.<sup>84,85</sup> Interestingly, in the presence of high levels of ectopic ZAP-70 from the AAV8-ZAP-70 vector (Fig 3, C), both the thymic and peripheral CD4/CD8 ratios in AAV8-ZAP-70-treated mice were significantly skewed to a CD4 lineage fate ( $P < .05$ ; Figs 2, D, and 3, E).

### Intrathymic AAV gene transfer results in development of T cells with integrated AAV8-ZAP-70 vectors and diverse $\alpha\beta$ TCR clonotypes

The persistence of gene-transduced T cells for more than 40 weeks was surprising in light of the high-level T-cell proliferation and the propensity of AAV vectors to remain episomal.<sup>86</sup> Therefore we first assessed vector copy numbers in peripheral T cells and determined that they ranged from approximately 0.1 to 1 vector genomes per diploid genome at time points ranging between 3 and 43 weeks after intrathymic gene transfer (Fig 4, A). The low copy number suggested that the vector was integrated, but to further assess this point, AAV8-ZAP-70-reconstituted T cells were TCR stimulated and copy numbers were evaluated. TCR-stimulated AAV8-ZAP-70-reconstituted T cells proliferated robustly, as monitored by using dilution of CellTrace Violet proliferation dye, demonstrating a reconstituted TCR signaling cascade (Fig 4, B). Moreover, although the vast majority of reconstituted T cells underwent more than 4 divisions, AAV copy number (vector genomes per diploid genome) was not significantly altered, strongly pointing to vector integration (Fig 4, B).

Genomic DNA was fragmented by means of sonication (to avoid biases caused by the nonrandom distribution of restriction sites on the genome), ligated to a barcoded linker cassette (LC) before PCR amplification, and evaluated through sonication linker-mediated PCR to directly assess vector integration. Nested PCR with vector- and LC-specific oligonucleotides allowed detection of PCR products with at least 2 different primers in lymph node samples from 3 of 6 intrathymic AAV8-ZAP-70-transduced mice (and 2 of 2 mice at 43 weeks after gene transfer; Fig 4, C). Thus integrated AAV is likely to be responsible for driving ZAP-70 expression in peripheral T cells under conditions of long-term persistence and TCR stimulation.

The potential of differentiated T cells to recognize a large array of foreign proteins is fostered by the unparalleled diversity of the TCR with recombinant  $\alpha$  and  $\beta$  polypeptide chains, allowing for the generation of more than  $10^{15}$  unique receptors.<sup>87</sup> However, under conditions of limited thymocyte differentiation, repertoire

diversity can be reduced.<sup>34</sup> Furthermore, infections and tumors can drive an antigen-mediated bias in  $\alpha\beta$  TCR repertoires.<sup>88</sup> Although only a few studies have monitored TCR repertoires in patients or mice treated with rAAV vectors, the robust T-cell response against an AAV transgene in one trial was shown to be associated with a biased TCRBV repertoire.<sup>89</sup> Therefore it was important to assess the repertoire diversity in our gene-corrected mice.

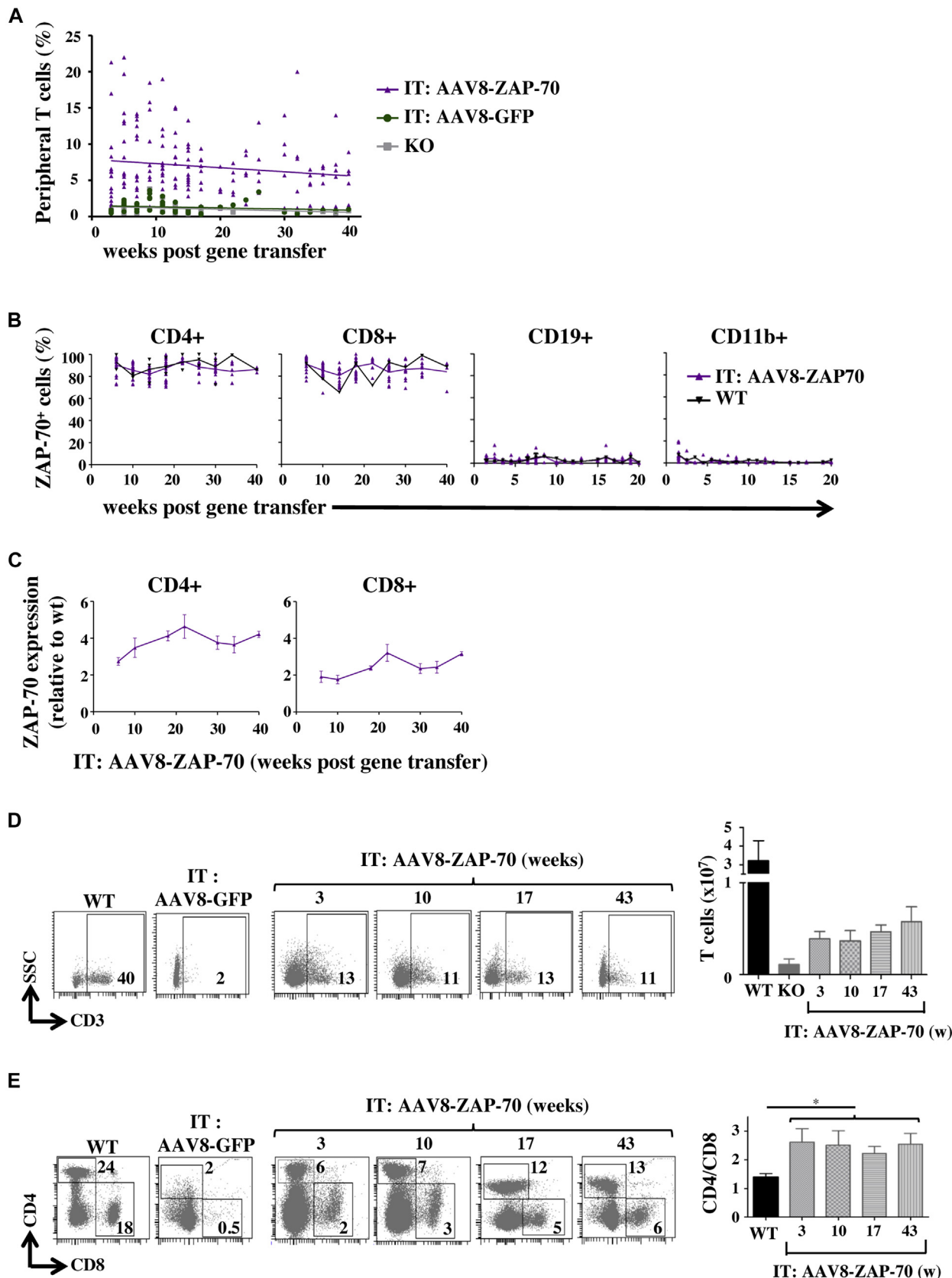
As expected, numbers of detected *Tra* sequences in both KO and AAV8-GFP-transduced mice were minimal; however, they increased rapidly after ZAP-70 gene transfer (day 10; Fig 4, D). TCR repertoire diversity was lower than that in WT mice, but the number of distinct *Trav*, *Traj*, *Trbv*, and *Trbj* clonotypes increased until 3 weeks after gene transfer and remained stable until 43 weeks (Fig 4, D). In WT mice clonotype distribution was not yet fully diverse at day 10 of life, being made up of a few mildly expanded TCRs. By week 3, WT mice exhibited repertoires that were fully diverse, with 1 to 3 copies per clonotype (Fig 4, D, bottom). The repertoires of AAV8-ZAP-70-reconstituted mice were less diverse than WT mice, with an expansion of some clonotypes, but a diverse population of TCRs was detected (Fig 4, D).

### Induction of humoral immunity in intrathymic AAV8-ZAP-70-treated mice

To determine whether AAV8-ZAP-70-transduced mice can mount an immune response, mice were immunized with OVA at a late time point after gene transfer (46 weeks). At this time point, neither WT nor KO mice harbored OVA-specific antibodies. Notably, however, mice that were intrathymically transduced with AAV8-ZAP-70 but not AAV8-GFP generated a significantly greater level of anti-OVA IgG antibodies by 6 weeks after immunization (1:2000 dilution,  $P < .001$ ; Fig 5, A). Although antibody generation was less than that detected in WT mice, AAV8-ZAP-70-transduced mice were already 1 year after gene transfer, and the level of IgG generation was highly significant relative to that of KO mice ( $P < .001$ ; Fig 5, A).

Changes in TCR repertoire distribution can result from immune responses against AAV capsid epitopes, as well as the expressed transgene.<sup>90</sup> Furthermore, different rAAV serotypes have induced T cell-dependent and independent anti-capsid humoral responses,<sup>91</sup> even when injected into an immune-privileged organ, such as the brain.<sup>92</sup> Therefore we monitored the presence of anti-capsid antibodies in intrathymic AAV8-treated ZAP-70<sup>-/-</sup> mice as a function of neutralization. Neutralizing factors were defined as serum dilutions that inhibited AAV8 infection by greater than 50%. No control ZAP-70<sup>-/-</sup>

**FIG 2.** Intrathymic AAV8-ZAP-70 gene transfer results in rapid reconstitution of the thymic architecture in ZAP-70<sup>-/-</sup> mice. **A**, Single-stranded AAV8-ZAP-70 or scAAV8-GFP virions were intrathymically injected into ZAP-70<sup>-/-</sup> (KO) mice, and thymi from WT, KO, and gene-transduced mice were evaluated for the presence of a thymic medulla by keratin 14 (K14) staining and AIRE<sup>+</sup> cells. Representative confocal images of thymic tissue sections at 1.5 (10 days), 3, and 10 weeks after gene transfer are shown. **B**, Numbers of AIRE<sup>+</sup> cells per square millimeter of thymus were quantified in the indicated conditions. Each point represents quantification of individual medulla derived from 3 distinct mice. **C**, Mean percentages of mature SP4 and SP8 thymocytes within the transduced GFP<sup>+</sup> and ZAP-70<sup>+</sup> subsets are shown in WT (left panel) and ZAP-70<sup>-/-</sup> (right panel) mice at the indicated time points after intrathymic AAV8-GFP and AAV8-ZAP-70 gene transfer, respectively. **D**, Absolute numbers of SP4 and SP8 thymocytes in WT mice (left panel) and AAV8-ZAP-70-transduced mice (right panel) were determined from the SP4 and SP8 gates at the indicated time points ( $n = 5$ ). Statistical significance was determined by using an unpaired 2-tailed *t* test or 1-way ANOVA with a Tukey multiple comparison test. *IT*, Intrathymic; *ns*, not significant. \* $P < .05$ , \*\* $P < .01$ , \*\*\* $P < .001$ , and \*\*\*\* $P < .0001$ .



mice harbored neutralizing antibodies, and at a 1:100 dilution, antibodies were not detected in intrathymic AAV8-ZAP-70-treated ZAP-70<sup>-/-</sup> mice. However, at a 1:10 dilution, 10 of 14 intrathymic AAV8-ZAP-70-treated ZAP-70<sup>-/-</sup> mice had positive results between 3 and 17 weeks after transduction (71%). Notably, however, at this dilution, anti-AAV8 neutralizing activity was also detected in a high percentage of intrathymic AAV8-GFP-treated ZAP-70<sup>-/-</sup> mice, mice that do not have peripheral T cells (4/5 [80%]; Fig 5, B). Thus intrathymic injection of the AAV8 serotype induces a low-level T cell-independent anti-capsid humoral response.

We next assessed whether the reconstituted mice exhibited an immune response against the ZAP-70 transgene. Intrathymic expression of the injected transgene likely minimizes an immune response, enhancing deletion of autoreactive thymocytes,<sup>33,35</sup> but our findings of a T cell-independent anti-capsid neutralizing activity (Fig 5, B) suggested the possibility of an anti-transgene response. Although anti-ZAP-70 antibodies were not detected at 3 weeks after AAV8-ZAP-70 transduction, 5 of 7 mice harbored antibodies at 10 weeks (>25 ng/mL sera;  $P < .01$ ). Mean antibody levels then decreased at 17 weeks (from 58 to 34 ng/mL), and by 43 weeks, antibody levels were less than 30 ng/mL ( $n = 5$ ; Fig 5, C), and ZAP-70 protein did not elicit T-cell activation (data not shown). In conclusion, anti-transgene antibodies were produced at early time points after intrathymic transduction, but levels decreased and were sufficiently low that they did not result in the elimination of gene-transduced T lymphocytes (Fig 2, B).

Patients with primary immunodeficiencies often present with autoimmune manifestations, and both immunodeficient patients and mice have been shown to produce a diverse range of autoantibodies.<sup>64,93</sup> Therefore we assessed whether gene-corrected ZAP-70<sup>-/-</sup> mice produced autoantibodies. Using an autoantigen microarray containing 123 different autoantigens, we did not observe increased levels of autoantibody production in age-matched ZAP-70<sup>-/-</sup> mice compared with control mice. However, intrathymic injections of both control AAV8-GFP and AAV8-ZAP-70 vectors resulted in induction of IgM antibodies against a broad panel of autoantigens by 3 weeks after gene transfer (see Fig E2 in this article's Online Repository at [www.jacionline.org](http://www.jacionline.org)). IgG antibody levels were significantly greater in intrathymic AAV8-ZAP-70-transduced mice in accord with the requirement of functional T cells for immunoglobulin class-switching. IgG autoantibodies peaked at 10 weeks after transduction (Fig 6, A).<sup>63,64</sup> Importantly, however, absolute levels of antibodies against 3 tested autoantigens (dsDNA, RNP, and SSA) were significantly lower in AAV8-ZAP-70-transduced

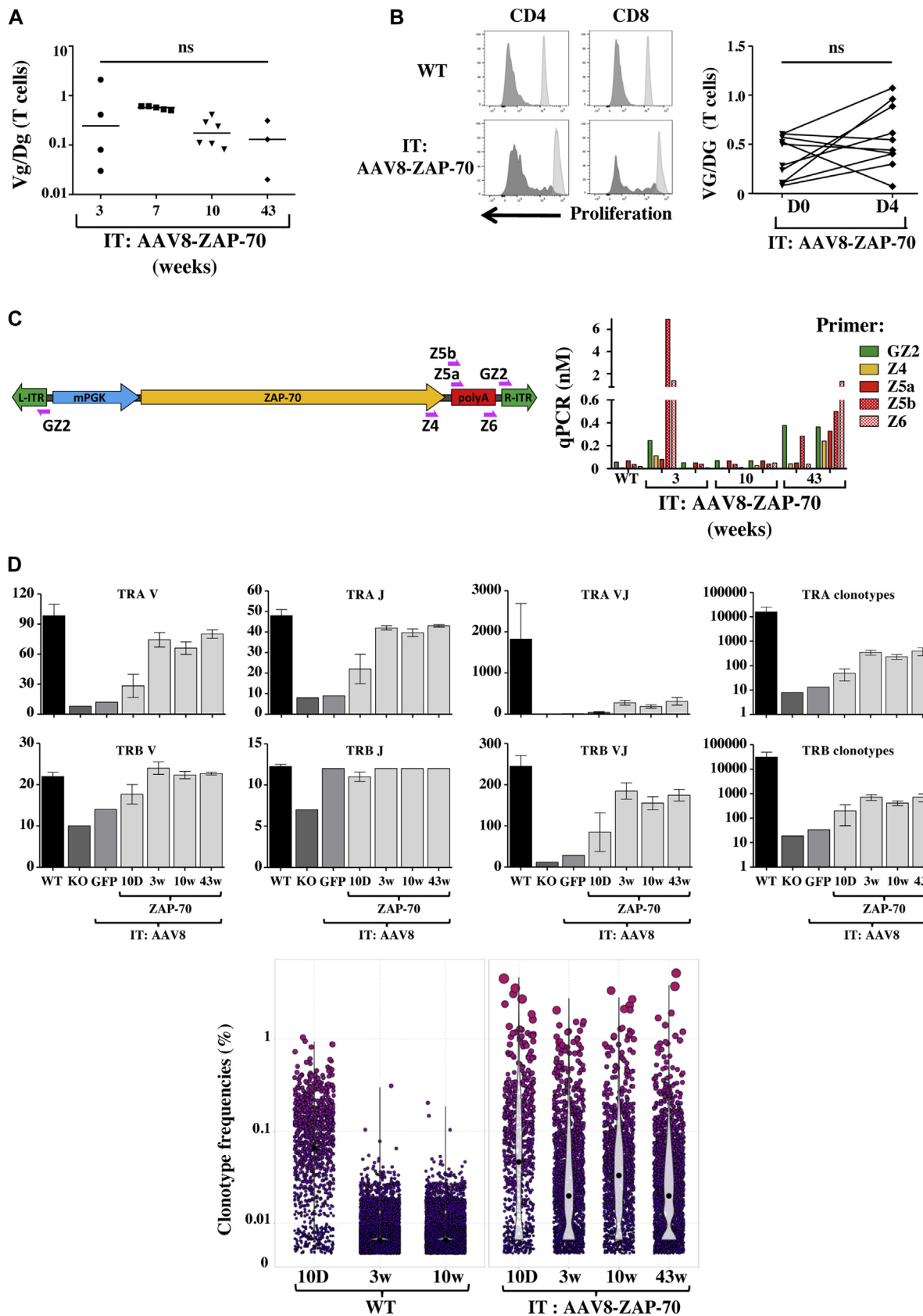
mice at both 10 and 43 weeks after gene transfer than in MRL/lpr mice, which spontaneously have a systemic lupus erythematosus-like syndrome. Furthermore, levels in AAV8-ZAP-70-transduced mice were not significantly greater than those detected in control MRL/MpJ mice (Fig 6, B). Thus intrathymic AAV8 administration induces a rapid but low-level broad spectrum of autoantibodies that decreases with time. Notably, these low levels of autoantibodies did not result in pathologic consequences because mice survived for more than 50 weeks without overt autoimmune manifestations.

### Intrathymic AAV8-ZAP-70 gene transfer results in differentiation of effector and regulatory T-cell subsets

Under conditions of lymphopenia, naive T cells proliferate in response to weak TCR interactions with self-peptide/MHC complexes, differentiating into memory-like T cells in the absence of antigenic stimulation.<sup>94</sup> Therefore it was important to study the phenotype of peripheral T cells in intrathymic AAV8-ZAP-70-reconstituted mice. Notably, reconstituted mice exhibited a significant increase in CD62L<sup>-</sup>CD44<sup>+</sup> effector memory T cells compared with the majority of CD62L<sup>+</sup>CD44<sup>-</sup> naive T cells in WT mice. This biased ratio of memory/naive T cells was detected throughout the experimental period of 10 months (Fig 7, A). Thus, in our study a single wave of thymocyte differentiation after intrathymic AAV8-ZAP-70 gene transfer resulted in peripheral differentiation of polyclonal T lymphocytes with a memory/effector phenotype.

To determine the potential effector function of AAV8-ZAP-70-transduced T cells, we first assessed *in vivo* cytokine levels. *In vivo* there was a transient increase in TNF- $\alpha$  and IFN- $\gamma$  levels at 3 weeks after AAV8 transduction (see Fig E3, A, in this article's Online Repository at [www.jacionline.org](http://www.jacionline.org)) correlating with induction of a low-level humoral response (Fig 6, A, and see Fig E2). However, cytokine levels then returned to baseline by 10 weeks (see Fig E3, A), which is consistent with the decrease in autoantibody levels. We next examined the ability of peripheral AAV8-ZAP70-reconstituted T cells to secrete cytokines on anti-CD3/anti-CD28 mAb activation. IL-17, TNF- $\alpha$ , and IFN- $\gamma$  were secreted by T cells from AAV8-ZAP-70-reconstituted mice by 3 weeks after gene transfer, and secretion of all 3 cytokines was significantly greater than that detected in KO mice by 10 weeks ( $n = 3-10$  mice per time point;  $P < .05$  and  $P < .001$ ; Fig 7, B). Compared with WT peripheral T cells, IL-17 was the only cytokine level that was significantly greater in gene-corrected mice ( $P < .05$ ; Fig 7, B). Thus peripheral

**FIG 3.** Intrathymic AAV8 transduction results in long-term maintenance of peripheral T cells and T lineage-specific transgene expression. **A**, The presence of peripheral blood T cells was monitored by using flow cytometry after intrathymic administration of AAV8-GFP or AAV8-ZAP-70 vectors, and data from individual mice are presented at 3 to 43 weeks. Statistical differences between mice treated with intrathymic AAV8-ZAP-70 gene transfer compared with those treated with intrathymic AAV8-GFP transfer or control KO mice were evaluated by using a 1-way ANOVA with a Tukey multiple comparison test for the following time groups: 3-10, 11-20, 21-30, and 31-40 weeks. \*\*\* $P < .001$  for all groups. **B**, Percentages of peripheral CD4<sup>+</sup>, CD8<sup>+</sup>, CD19<sup>+</sup>, and CD11b<sup>+</sup> hematopoietic cells expressing ectopic ZAP-70 after intrathymic AAV8-ZAP-70 transduction are presented. **C**, ZAP-70 protein expression in transduced T cells evaluated by using intracellular staining and mean fluorescence intensity relative to WT T cells are presented at the indicated time points. **D**, Representative plots of CD3<sup>+</sup> lymph node T cells are presented. Total T-cell numbers (means  $\pm$  SEMs) are shown (right). **E**, Repartition of CD4/CD8 lymphocytes and mean CD4/CD8 ratios are shown at the indicated time points. Statistical significance was determined by using a 2-tailed unpaired *t* test. \* $P < .05$ . *IT*, Intrathymic; *SSC*, side scatter.



AAV8-ZAP-70-reconstituted T cells were competent to secrete cytokines after *ex vivo* TCR stimulation.

Despite high *ex vivo* TCR-induced cytokine secretion, *in vivo* cytokine levels were not increased, and AAV-reconstituted mice did not exhibit autoimmune symptoms. Therefore it was important to assess whether gene-corrected regulatory T (Treg) cells controlled immune responsiveness in these mice. Notably, development of Treg cells expressing the FOXP3 transcription factor is dependent on a thymic medulla,<sup>95</sup> a structure that was restored by day 10 of gene transfer (Fig 2, A). Accordingly, by 3 weeks after gene transfer, Treg cells were detected in the peripheral circulation of AAV8-ZAP-70-treated mice at levels similar to those in WT mice (Fig 7, C). Notably, by 10 weeks after intrathymic gene transfer, Treg cell percentages were significantly greater in AAV8-ZAP-70-treated mice than in WT mice ( $P < .05$ ; Fig 7, C). Importantly, these T cells exhibited an activated phenotype, as monitored by significantly greater levels of Treg cell markers, including cytotoxic T lymphocyte-associated antigen 4 (CTLA4), glucocorticoid-induced TNFR family related gene (GITR), and CD39 ( $n = 5$  per group; see Fig E3, B).

Regarding function, sorted CD4<sup>+</sup>CD25<sup>hi</sup> cells from both WT and AAV8-ZAP-70-transduced cells revealed equivalent levels of *Foxp3* transcripts ( $n = 12$ ), but *Il10* levels were significantly greater in the latter ( $P < .05$ ; Fig 7, D). Furthermore, *Il10* expression was significantly greater in conventional (CD4<sup>+</sup>CD25<sup>-</sup>) T cells from reconstituted mice than from WT mice ( $n = 6-9$ ,  $P < .005$ ). Thus a high suppressive environment in reconstituted Treg cells likely restrains *in vivo* immune activation after AAV8-ZAP-70 gene transfer.

## DISCUSSION

Thymocyte development is dependent on the thymic stroma, which is composed of TECs and nonepithelial cells that together form an organized 3-dimensional network.<sup>96</sup> Intercellular communications between developing thymocytes and TECs result in a thymus architecture that allows generation of a diverse and self-tolerant pool of mature T cells. In patients with SCID, as well as patients with cancer with thymus damage, an abnormal thymic architecture negatively affects thymocyte differentiation.<sup>19,65,66,97</sup> Here we show that an intrathymic AAV8 gene correction results in a remarkable generation of mTECs and development of a medullary architecture in ZAP-70-deficient mice within 10 days of vector administration. Moreover, the absolute number of mTECs expressing AIRE increased by 3-fold in this period. AIRE is critical for immune tolerance, promoting deletion of self-reactive thymocytes and development of Treg

cells.<sup>65,66,68,69</sup> Therefore, to date, the intrathymic AAV gene transfer strategy described here appears to be the most rapid regulator of thymic architecture in immunodeficient mice.

Because cross-talk between mTECs and developing thymocytes is required for T-cell maturation, extensive research has focused on identification of factors, conditions, and cell types that enhance mTEC reconstitution.<sup>98</sup> Differentiation of autoreactive mature CD4 thymocytes regulates the formation and organization of the medulla in an antigen-dependent manner, as shown by the importance of the CD28-CD80/CD86 and CD40-CD40 ligand costimulatory pathways, as well as receptor activator of nuclear factor  $\kappa$ B (RANK)-receptor activator of nuclear factor  $\kappa$ B ligand (RANKL) and lymphotoxin  $\alpha\beta$ -lymphotoxin  $\beta$  receptor interactions.<sup>68</sup> Furthermore, sex steroid ablation was found to enhance thymocyte differentiation by increasing Notch ligand expression on TECs,<sup>99-101</sup> whereas keratinocyte growth factor, IL-22, BMP4, and FOXN1 directly promote TEC proliferation and survival.<sup>102-104</sup> Specific cell types, such as pro-T cells, facilitate thymus reconstruction,<sup>32,105,106</sup> whereas innate lymphoid cells induce IL-22-mediated TEC survival.<sup>107</sup> Chemokines can also facilitate thymic reconstitution; under conditions of thymic damage, CCL21 treatment of hematopoietic progenitors rescues their migration, whereas combined inhibition of p53 and keratinocyte growth factor increases intrathymic CCL21 expression and TEC recovery.<sup>29,108</sup> Notably, however, the success of these approaches often requires a significant lag time, whereas an intrathymic AAV gene strategy corrected the medullary microenvironment within less than 10 days, which is concomitant with a correction in T-cell deficiency and differentiation of SP4 thymocytes. It will be of interest to determine whether a combined approach, concomitantly correcting a T-cell deficiency and the medullary microenvironment,<sup>59</sup> further promotes reconstitution. Furthermore, AAV can be used to deliver TEC-inducing molecules to patients with suboptimal T-cell differentiation (eg, boosting thymocyte differentiation in HSC-transplanted patients with cancer by means of intrathymic AAV administration of the IL-22 cytokine). This type of intrathymic targeting approach, using ultrasound-mediated guidance, has been shown to be minimally invasive and safe in both mice and macaques.<sup>28,31,37,109</sup> Further studies focused on intrathymic administration of vectors and hematopoietic progenitor cells into nonhuman primates by interventional radiologists will help to establish the clinical framework in which this type of therapeutic strategy can be developed.

AAV vectors have successfully been used to achieve gene transfer in numerous tissues.<sup>81</sup> Nevertheless, studies of AAV gene transfer in the hematopoietic system have been more

**FIG 4.** AAV8-ZAP-70-transduced peripheral T lymphocytes exhibit stable vector genomes after TCR-induced proliferation and diverse TCR repertoires. **A**, AAV genome copy numbers in lymph node samples were assessed by using qPCR in intrathymic AAV8-ZAP-70-transduced mice at the indicated time points. Vector genomes per diploid genome (*Vg/Dg*) were quantified relative to the albumin gene and normalized to T-cell percentages. **B**, Proliferation was assessed after TCR stimulation by using CellTrace Violet fluorescence, and representative histograms at day 0 (light gray) and day 4 (dark gray) are shown. AAV genome copy was monitored as above, and quantifications ( $n = 9$ ) are shown. **C**, Schematic representation of the AAV-ZAP-70 vector are shown. PCR products, representing an integrated vector, are shown at the indicated time points, and T cells from WT mice are presented as a negative control. **D**, Numbers of distinct *Trav*, *Traj*, *Travj*, *Trbv*, *Trbj*, *Trbvj*, *Tra*, and *Trb* clonotypes are presented (top). Clonotype frequencies are presented, with each clonotype represented by a dot, the size of which is proportional to its frequency. Violin plots represent the density of the distribution, and black dots show the median frequency per repertoire (bottom). *IT*, Intrathymic; *ns*, not significant.

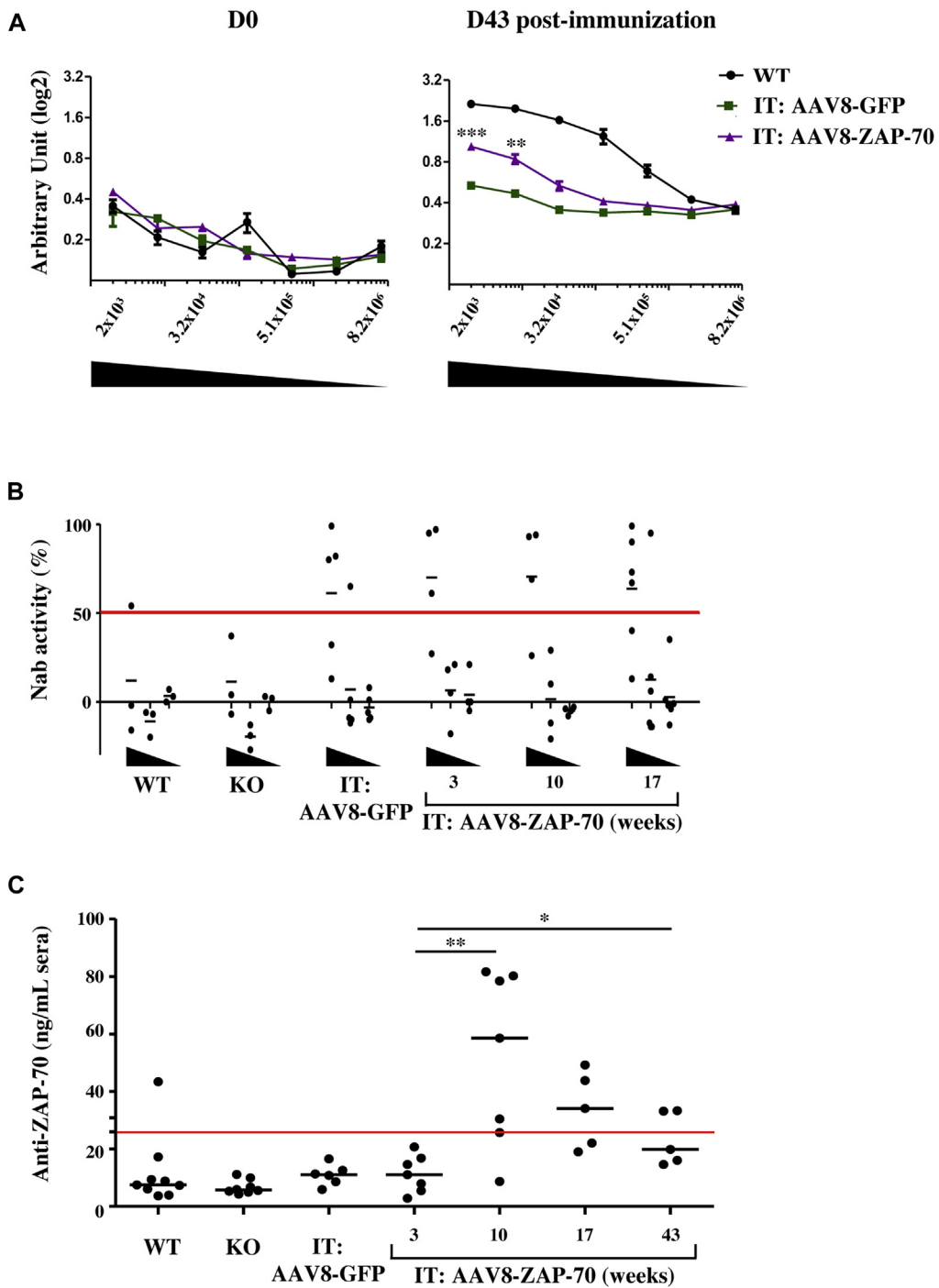


**FIG 5.** Induction of a T cell-independent humoral response to AAV8 capsid epitopes after intrathymic vector administration. **A**, Total IgG titers against OVA were monitored in nonimmunized WT, KO, and intrathymic AAV8-ZAP-70-treated KO mice (46 weeks after gene transfer) and 6 weeks after immunization by means of ELISA. Reactivity was monitored as a function of dilution, as indicated ( $n = 4$ ). Statistical significance was evaluated at each dilution by using a 1-way ANOVA with a Tukey multiple comparison test for each dilution and is noted for significant differences. **B**, Neutralizing antibodies (Nab) against the AAV8 serotype were monitored in WT and ZAP-70<sup>-/-</sup> mice after intrathymic AAV8-GFP and AAV8-ZAP-70 transduction. Serum dilutions of 1:10, 1:100, and 1:1000 are shown by the decreasing slope of the triangle, respectively, and Nab activity is defined as a decrease in AAV transduction of greater than 50% compared with AAV incubation with PBS alone (red line). Each point represents serum from an individual mouse at 3, 10, and 17 weeks after transduction, and mean levels are indicated by a horizontal line. **C**, Antibodies against ZAP-70 protein were measured by using an ELISA, and data are presented as nanograms of antibody per milliliter of serum. Antibody levels of greater than 25 ng/mL are considered significant. \* $P < .05$ , \*\* $P < .01$ , and \*\*\* $P < .001$ .

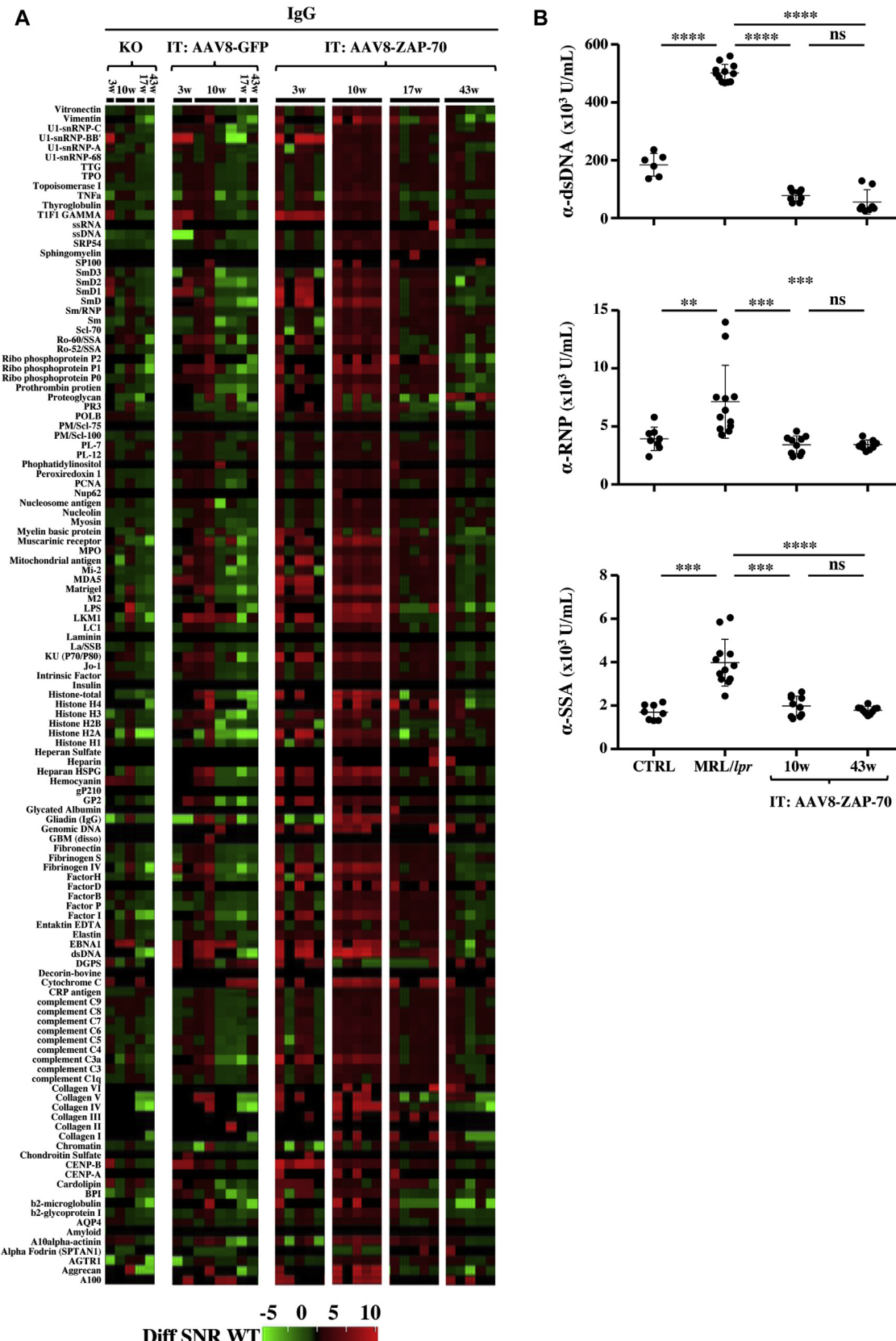
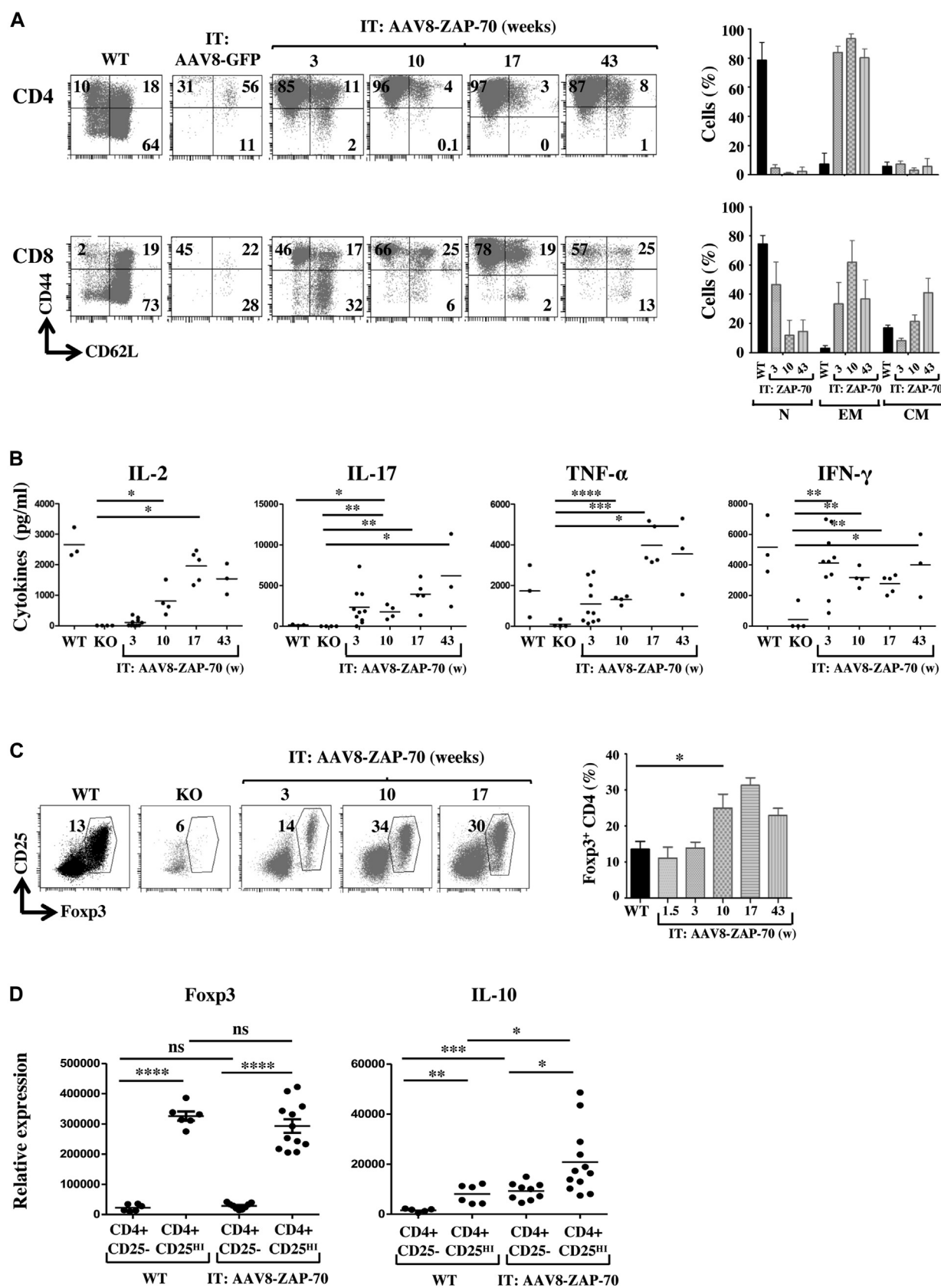


**FIG 6.** Transient induction of a broad spectrum of antibodies in ZAP-70 $^{-/-}$  mice after intrathymic AAV8 gene transfer remains significantly lower than that detected in autoimmune mice. **A**, The presence of IgG autoantibodies in serum samples of ZAP-70 $^{-/-}$  (KO) mice and after intrathymic administration of either AAV8-GFP or AAV8-ZAP-70 vectors was evaluated at the indicated time points. IgG autoantibodies against 123 antigens were assessed by using a protein microarray, and heat maps showing autoantibody reactivity relative to levels in age-matched WT mice are presented. **B**, Levels of autoantibodies against RNP, dsDNA, and SSA were evaluated by means of ELISA in control MRL/MpJ mice, autoimmune-prone MRL/lpr mice, and intrathymic AAV8-ZAP-70-treated mice at 10 and 43 weeks after gene transfer. Each point represents serum from an individual mouse. Statistical significance was determined by using a 1-way ANOVA with a Tukey multiple comparison test. \*\*\* $P$  < .01, \*\*\* $P$  < .001, and \*\*\*\* $P$  < .0001. IT, Intrathymic; ns, not significant; SNR, signal to noise ratio.



sparse, likely because of the extensive division of these cells. However, AAV1, modified AAV6, and AAV7 vectors have been found to efficiently transduce HSCs.<sup>54,57,110,111</sup> Furthermore, we show here that AAV8, AAV9, and AAV10 serotypes promote efficient thymocyte transduction. Although the properties of AAV vector genomes to exist primarily as episomes would be expected to negatively affect their ability to be used for stable gene therapy in dividing cells, long-term persistence of transgene expression has been detected in HSCs.<sup>54,55,57</sup>

Moreover, it has recently been shown that T lymphocytes represent the *in vivo* site of AAV persistence after natural infection.<sup>112</sup> This is likely linked to the AAV vector-mediated long-term transgene maintenance (>10 months) that we detected in gene-corrected T lymphocytes. Indeed, our findings that AAV vector copy number in reconstituted T cells was approximately 1 and that long-term reconstituted T cells harbored integrated vector is likely to broaden the scope of immunologic deficiencies for which this type of approach can be envisioned. Because the persistence of intrathymic injected progenitors with a specific TCR gene provided for life-long immunity,<sup>31</sup> it will be of interest to determine whether direct targeting of thymocytes with an AAV8-encoded tumor-specific TCR or chimeric antigen receptor will promote an antitumor response that is superior to that currently achieved by means of *ex vivo* manipulation of peripheral T cells.

Immune responses against AAV capsid serotypes, as well as expressed transgenes, have hampered the success of AAV gene therapy trials.<sup>113</sup> Anti-capsid antibodies have been detected even after AAV injections into regions that are considered to be immune privileged, such as the brain<sup>92</sup> or intraventricular space.<sup>114,115</sup> Nevertheless, the development of immunosuppressive treatments has protected against AAV capsid immunity.<sup>116-118</sup> Indeed, long-term transgene expression has been observed after systemic AAV administration of genes, such as myotubularin<sup>119,120</sup> and microdystrophin,<sup>121</sup> promoting AAV-based treatments for patients with X-linked myotubular myopathy and Duchenne muscular dystrophy, respectively.

Although T-cell immunity can provoke anti-AAV reactivity, it can also limit pathologic responses. Recruitment of suppressive Treg cells, as well as organ-specific T-cell exhaustion, can result in extended transgene expression.<sup>122,123</sup> Although we initially hypothesized that direct administration of AAV into the thymus would result in deletion of autoreactive thymocytes and the subsequent absence of an immune response,<sup>33,35</sup> we detected low-level humoral responses to both the AAV8 capsid and the ZAP-70 transgene. Interestingly, anti-capsid responses were induced at similar levels in ZAP-70<sup>-/-</sup> mice treated with intrathymic

administration of the control AAV8-GFP vector. Because T-cell differentiation did not proceed in these latter mice, these data indicate the development of a T cell-independent immune response. In contrast, IgG autoantibodies were generated in AAV gene-corrected ZAP-70<sup>-/-</sup> mice, pointing to the importance of T cells in immunoglobulin class-switching. Moreover, similarly to patients in whom AAV transduction correlated with increases in specific TCRBV families,<sup>122</sup> the humoral immune response in intrathymic AAV8-ZAP-70-treated mice was associated with a diverse but biased TCR repertoire. Notably, however, levels of generated autoantibodies were significantly lower than those detected in systemic lupus erythematosus-prone MRL/lpr mice, and none of the intrathymic gene therapy-treated mice had symptoms of autoimmune disease during the 10-month follow-up period. This is likely due to (1) the low and transient nature of the autoantibody response and (2) the extensive differentiation of AAV-corrected thymocytes to a Treg cell fate. Notably, AAV gene transfer resulted in an effector T-cell/Treg cell ratio that allowed for balanced immune homeostasis.

Combination therapies will likely optimize life-long T-cell differentiation in patients with SCID and T-cell reconstitution in patients with cancer. An ideal treatment will promote (1) HSC expansion, (2) migration and entry of hematopoietic progenitors into the thymus, (3) a thymus architecture that is conducive to thymocyte maturation, and (4) selection of a broad-based repertoire of self-tolerant effector and Treg cells. One bottleneck is progenitor entry because the thymus is not continually receptive to the importance of hematopoietic progenitors, at least in mice.<sup>124,125</sup> Furthermore, irradiation reduces progenitor homing by more than 10-fold.<sup>29</sup> Although this bottleneck can be partially overcome by injecting HSCs or hematopoietic progenitors directly into the thymus,<sup>24,27,28,31,109,126,127</sup> histocompatible donors are not always available. Our study reveals the potential of an intrathymic AAV8 gene therapy strategy to promote extremely rapid reconstitution of the thymus microenvironment and the differentiation of mTEC-dependent Treg cells within a 7- to 10-day period.

In our studies a single wave of thymocyte differentiation promoted long-term maintenance of peripheral gene-corrected T cells. Indeed, in several “experiments of nature,” patients with mutations that generally result in an SCID phenotype were found to be relatively healthy, with significant T-cell numbers caused by a reversion mutation. Because this type of event is statistically improbable, it is likely that the peripheral T-cell reconstitution detected in these patients (with mutations in WAS, RAG1, LAD, NEMO, CD3 $\zeta$ ,  $\gamma$ c, and ADA) is due to a reversion mutation in a single hematopoietic progenitor.<sup>128-140</sup> Although these data strongly support the hypothesis that gene correction of a very limited number of thymic progenitors can give rise to a large

**FIG 7.** AAV8-ZAP-70-transduced thymocytes differentiate into effector T and Treg cells. **A**, The presence of naïve (CD62L $^{+}$ CD44 $^{-}$ ; *N*), central memory (CD62L $^{+}$ CD44 $^{+}$ ; *CM*), and effector memory (CD62L $^{-}$ CD44 $^{+}$ ; *EM*) cells within the CD4 and CD8 subsets were monitored at 3, 10, 17, and 43 weeks after intrathymic AAV8-ZAP-70 gene transfer. Percentages of cells in each subset were quantified at each time point, and mean  $\pm$  SEM levels ( $n = 4-5$  mice per time point) are presented. **B**, Lymph node cells from the indicated mice were stimulated *ex vivo* with anti-CD3/anti-CD28 mAbs for 3 days, and cytokine secretion was measured. Each point represents data from a single mouse, and horizontal lines represent mean levels (in picograms per milliliter). **C**, Percentages of FOXP3 $^{+}$ CD25 $^{+}$  peripheral Treg cells were evaluated, and representative dot plots are presented (*left*) together with mean  $\pm$  SEM percentages at each time point ( $n = 5-14$  mice per time point, *right*). **D**, Conventional and Treg CD4 cell subsets were FACS sorted on the basis of CD25 expression. *Foxp3* and *Il10* transcripts in each subset were monitored by using quantitative RT-PCR ( $n = 2-4$  mice in 2 independent experiments). Statistical significance was determined by using a 2-tailed unpaired *t* test. \**P* < .05, \*\**P* < .01, \*\*\**P* < .001, and \*\*\*\**P* < .0001. *IT*, Intrathymic; *ns*, not significant.

number of peripheral T cells, it remains to be determined whether T cells in these patients are due to a single wave of thymocyte differentiation. Moreover, in the context of an intrathymic gene transfer approach, it will be important to assess whether the remnant thymus present in many patients with SCID, as well as the natural process of thymic involution, would negatively affect the type of therapeutic strategy described here. Importantly, we found that intrathymic gene transfer into RAG2<sup>-/-</sup> mice with a remnant thymus is feasible through a surgical approach, but the success of intrathymic HSC transfer into older mice with an involuted thymus is significantly reduced (our unpublished observations). Thus a combination therapy of intrathymic AAV gene transfer, promoting restoration of the thymic architecture and medulla formation, followed by an intravenous HSC transplantation allowing long-term T-cell differentiation in a reconstituted thymus, might present a novel approach for the treatment of immunodeficient patients requiring a rapid T-cell reconstitution.

We thank all members of our laboratory for their scientific critique and support. The authors thank the Center for Production of Vector (CPV-vector core from University Hospital of Nantes, French Institute of Health [INSERM], University of Nantes; <http://umr1089.univ-nantes.fr/plateaux-technologiques/cpv/centre-de-production-de-vecteurs-2194757.kjsp?RH=1518531897125>) and are grateful to Myriam Boyer of Montpellier Rio Imaging for support in cytometry experiments, Léo Garcia for his assistance in bioinformatic analyses, and Luz Blanco and Mariana Kaplan for generously providing serum from autoimmune MRL/lpr mice and providing advice on ELISAs and the ZEFI staff for their support of animal experiments.

### Key messages

- **Intrathymic AAV gene correction of an immunodeficiency promotes the differentiation of normal thymic architecture within 10 days after gene transfer.**
- **Intrathymic AAV gene transfer results in vector integration with the persistence of gene-corrected peripheral T cells for more than 40 weeks.**

### REFERENCES

1. Al-Herz W, Bousfiha A, Casanova JL, Chatila T, Conley ME, Cunningham-Rundles C, et al. Primary immunodeficiency diseases: an update on the classification from the international union of immunological societies expert committee for primary immunodeficiency. *Front Immunol* 2014;5:162.
2. Heimall J, Puck J, Buckley R, Fleisher TA, Gennery AR, Neven B, et al. Current knowledge and priorities for future research in late effects after hematopoietic stem cell transplantation (HCT) for severe combined immunodeficiency patients: a consensus statement from the Second Pediatric Blood and Marrow Transplant Consortium International Conference on Late Effects after Pediatric HCT. *Biol Blood Marrow Transplant* 2017;23:379-87.
3. Fischer A, Hacein-Bey-Abina S, Cavazzana-Calvo M. Gene therapy for primary immunodeficiencies. *Hematol Oncol Clin North Am* 2011;25:89-100.
4. Aiuti A, Cattaneo F, Galimberti S, Benninghoff U, Cassani B, Callegaro L, et al. Gene therapy for immunodeficiency due to adenosine deaminase deficiency. *N Engl J Med* 2009;360:447-58.
5. Aiuti A, Biasco L, Scaramuzza S, Ferrua F, Ciealese MP, Baricordi C, et al. Lentiviral hematopoietic stem cell gene therapy in patients with Wiskott-Aldrich syndrome. *Science* 2013;341:1233151.
6. Mukherjee S, Thrasher AJ. Gene therapy for PIDs: progress, pitfalls and prospects. *Gene* 2013;525:174-81.
7. Fischer A, Hacein-Bey-Abina S, Cavazzana-Calvo M. Gene therapy of primary T cell immunodeficiencies. *Gene* 2013;525:170-3.
8. Hacein-Bey Abina S, Gaspar HB, Blonseau J, Caccavelli L, Charrier S, Buckland K, et al. Outcomes following gene therapy in patients with severe Wiskott-Aldrich syndrome. *JAMA* 2015;313:1550-63.
9. Pala F, Morbach H, Castiello MC, Schickel JN, Scaramuzza S, Chamberlain N, et al. Lentiviral-mediated gene therapy restores B cell tolerance in Wiskott-Aldrich syndrome patients. *J Clin Invest* 2015;125:3941-51.
10. Castiello MC, Scaramuzza S, Pala F, Ferrua F, Uva P, Brigida I, et al. B-cell reconstitution after lentiviral vector-mediated gene therapy in patients with Wiskott-Aldrich syndrome. *J Allergy Clin Immunol* 2015;136:692-702.e2.
11. Shaw KL, Garabedian E, Mishra S, Barman P, Davila A, Carbonaro D, et al. Clinical efficacy of gene-modified stem cells in adenosine deaminase-deficient immunodeficiency. *J Clin Invest* 2017;127:1689-99.
12. Aiuti A, Roncarolo MG, Naldini L. Gene therapy for ADA-SCID, the first marketing approval of an ex vivo gene therapy in Europe: paving the road for the next generation of advanced therapy medicinal products. *EMBO Mol Med* 2017;9:737-40.
13. Thrasher AJ, Gaspar HB, Baum C, Modlich U, Schambach A, Candotti F, et al. Gene therapy: X-SCID transgene leukaemogenicity. *Nature* 2006;443:E5-7.
14. Hacein-Bey-Abina S, Garrigue A, Wang GP, Soulier J, Lim A, Morillon E, et al. Insertional oncogenesis in 4 patients after retrovirus-mediated gene therapy of SCID-X1. *J Clin Invest* 2008;118:3132-42.
15. Howe SJ, Mansour MR, Schwarzwälder K, Bartholomae C, Hubank M, Kempki H, et al. Insertional mutagenesis combined with acquired somatic mutations causes leukemogenesis following gene therapy of SCID-X1 patients. *J Clin Invest* 2008;118:3143-50.
16. Stein S, Ott MG, Schultz-Strasser S, Jauch A, Burwinkel B, Kinner A, et al. Genomic instability and myelodysplasia with monosomy 7 consequent to EVI1 activation after gene therapy for chronic granulomatous disease. *Nat Med* 2010;16:198-204.
17. De Ravin SS, Wu X, Moir S, Anaya-O'Brien S, Kwatemaa N, Littel P, et al. Lentiviral hematopoietic stem cell gene therapy for X-linked severe combined immunodeficiency. *Sci Transl Med* 2016;8:335ra57.
18. Mamcarz E, Zhou S, Lockey T, Abdelsamed H, Cross SJ, Kang G, et al. Lentiviral gene therapy combined with low-dose busulfan in infants with SCID-X1. *N Engl J Med* 2019;380:1525-34.
19. Shah DK, Zuniga-Pflucker JC. An overview of the intrathymic intricacies of T cell development. *J Immunol* 2014;192:4017-23.
20. Goldschneider I, Komschlies KL, Greiner DL. Studies of thymocytopenia in rats and mice. I. Kinetics of appearance of thymocytes using a direct intrathymic adoptive transfer assay for thymocyte precursors. *J Exp Med* 1986;163:1-17.
21. Scollay R, Smith J, Stauffer V. Dynamics of early T cells: prothymocyte migration and proliferation in the adult mouse thymus. *Immunol Rev* 1986;91:129-57.
22. Frey JR, Ernst B, Surh CD, Sprent J. Thymus-grafted SCID mice show transient thymopoiesis and limited depletion of V beta 11+ T cells. *J Exp Med* 1992;175:1067-71.
23. Berzins SP, Boyd RL, Miller JF. The role of the thymus and recent thymic migrants in the maintenance of the adult peripheral lymphocyte pool. *J Exp Med* 1998;187:1839-48.
24. Vicente R, Adjali O, Jacquet C, Zimmermann VS, Taylor N. Intrathymic transplantation of bone marrow-derived progenitors provides long-term thymopoiesis. *Blood* 2010;115:1913-20.
25. Martins VC, Ruggiero E, Schlenner SM, Madan V, Schmidt M, Fink PJ, et al. Thymus-autonomous T cell development in the absence of progenitor import. *J Exp Med* 2012;209:1409-17.
26. Peaudecerf L, Lemos S, Galgano A, Krenn G, Vasseur F, Di Santo JP, et al. Thymocytes may persist and differentiate without any input from bone marrow progenitors. *J Exp Med* 2012;209:1401-8.
27. de Barros SC, Zimmermann VS, Taylor N. Concise review: hematopoietic stem cell transplantation: targeting the thymus. *Stem Cells* 2013;31:1245-51.
28. Tuckett AZ, Thornton RH, O'Reilly RJ, van den Brink MRM, Zakrzewski JL. Intrathymic injection of hematopoietic progenitor cells establishes functional T cell development in a mouse model of severe combined immunodeficiency. *J Hematol Oncol* 2017;10:109.
29. Zhang SL, Wang X, Manna S, Zlotoff DA, Bryson JL, Blazar BR, et al. Chemo-kinetic treatment rescues profound T-lineage progenitor homing defect after bone marrow transplant conditioning in mice. *Blood* 2014;124:296-304.
30. Thordardottir S, Hangalapura BN, Hutten T, Cossu M, Spanholz J, Schaap N, et al. The aryl hydrocarbon receptor antagonist StemRegenin 1 promotes human plasmacytoid and myeloid dendritic cell development from CD34+ hematopoietic progenitor cells. *Stem Cells Dev* 2014;23:955-67.
31. Tuckett AZ, Thornton RH, Shono Y, Smith OM, Levy ER, Kreines FM, et al. Image-guided intrathymic injection of multipotent stem cells supports lifelong T-cell immunity and facilitates targeted immunotherapy. *Blood* 2014;123:2797-805.
32. Smith MJ, Reichenbach DK, Parker SL, Riddle MJ, Mitchell J, Osum KC, et al. T cell progenitor therapy-facilitated thymopoiesis depends upon thymic input and continued thymic microenvironment interaction. *JCI Insight* 2017;2.

33. DeMatteo RP, Chu G, Ahn M, Chang E, Barker CF, Markmann JF. Long-lasting adenovirus transgene expression in mice through neonatal intrathymic tolerance induction without the use of immunosuppression. *J Virol* 1997;71:5330-5.
34. Adjali O, Marodon G, Steinberg M, Mongellaz C, Thomas-Vaslin V, Jacquet C, et al. In vivo correction of ZAP-70 immunodeficiency by intrathymic gene transfer. *J Clin Invest* 2005;115:2287-95.
35. Marodon G, Fisson S, Levacher B, Fabre M, Salomon BL, Klatzmann D. Induction of antigen-specific tolerance by intrathymic injection of lentiviral vectors. *Blood* 2006;108:2972-8.
36. Irla M, Saade M, Kissenseppen A, Poulin LF, Leserman L, Marche PN, et al. ZAP-70 restoration in mice by *in vivo* thymic electroporation. *PLoS One* 2008;3:e2059.
37. Moreau A, Vicente R, Dubreil L, Adjali O, Podevin G, Jacquet C, et al. Efficient intrathymic gene transfer following *in situ* administration of a rAAV serotype 8 vector in mice and nonhuman primates. *Mol Ther* 2009;17:472-9.
38. Le Bec C, Douar AM. Gene therapy progress and prospects—vectorology: design and production of expression cassettes in AAV vectors. *Gene Ther* 2006;13:805-13.
39. Russell DW. AAV vectors, insertional mutagenesis, and cancer. *Mol Ther* 2007;15:1740-3.
40. Buning H, Huber A, Zhang L, Meumann N, Hacker U. Engineering the AAV capsid to optimize vector-host-interactions. *Curr Opin Pharmacol* 2015;24:94-104.
41. Brown N, Song L, Kollu NR, Hirsch ML. Adeno-associated virus vectors and stem cells: friends or foes? *Hum Gene Ther* 2017;28:450-63.
42. Chandler RJ, Sands MS, Venditti CP. Recombinant adeno-associated viral integration and genotoxicity: insights from animal models. *Hum Gene Ther* 2017;28:314-22.
43. Kaplitt MG, Leone P, Samulski RJ, Xiao X, Pfaff DW, O'Malley KL, et al. Long-term gene expression and phenotypic correction using adeno-associated virus vectors in the mammalian brain. *Nat Genet* 1994;8:148-54.
44. Kaplitt MG, Xiao X, Samulski RJ, Li J, Ojamaa K, Klein IL, et al. Long-term gene transfer in porcine myocardium after coronary infusion of an adeno-associated virus vector. *Ann Thorac Surg* 1996;62:1669-76.
45. McCown TJ, Xiao X, Li J, Breese GR, Samulski RJ. Differential and persistent expression patterns of CNS gene transfer by an adeno-associated virus (AAV) vector. *Brain Res* 1996;713:99-107.
46. Griffey MA, Wozniak D, Wong M, Bible E, Johnson K, Rothman SM, et al. CNS-directed AAV2-mediated gene therapy ameliorates functional deficits in a murine model of infantile neuronal ceroid lipofuscinosis. *Mol Ther* 2006;13:538-47.
47. Sondhi D, Peterson DA, Giannaris EL, Sanders CT, Mendez BS, De B, et al. AAV2-mediated CLN2 gene transfer to rodent and non-human primate brain results in long-term TPP-I expression compatible with therapy for LINCL. *Gene Ther* 2005;12:1618-32.
48. Xiao X, Li J, McCown TJ, Samulski RJ. Gene transfer by adeno-associated virus vectors into the central nervous system. *Exp Neurol* 1997;144:113-24.
49. Hargrove PW, Vanin EF, Kurtzman GJ, Nienhuis AW. High-level globin gene expression mediated by a recombinant adeno-associated virus genome that contains the 3' gamma globin gene regulatory element and integrates as tandem copies in erythroid cells. *Blood* 1997;89:2167-75.
50. Malik P, McQuiston SA, Yu XJ, Pepper KA, Krall WJ, Podskaloff GM, et al. Recombinant adeno-associated virus mediates a high level of gene transfer but less efficient integration in the K562 human hematopoietic cell line. *J Virol* 1997;71:1776-83.
51. Nathwani AC, Hanawa H, Vandergriff J, Kelly P, Vanin EF, Nienhuis AW. Efficient gene transfer into human cord blood CD34+ cells and the CD34+CD38- subset using highly purified recombinant adeno-associated viral vector preparations that are free of helper virus and wild-type AAV. *Gene Ther* 2000;7:183-95.
52. Schuhmann NK, Pozzoli O, Sallach J, Huber A, Avitabile D, Perabo L, et al. Gene transfer into human cord blood-derived CD34(+) cells by adeno-associated viral vectors. *Exp Hematol* 2010;38:707-17.
53. Veldwijk MR, Sellner L, Stielhofen M, Kleinschmidt JA, Laufs S, Topaly J, et al. Pseudotyped recombinant adeno-associated viral vectors mediate efficient gene transfer into primary human CD34(+) peripheral blood progenitor cells. *Cytotherapy* 2010;12:107-12.
54. Song L, Kauss MA, Kopin E, Chandra M, Ul-Hasan T, Miller E, et al. Optimizing the transduction efficiency of capsid-modified AAV6 serotype vectors in primary human hematopoietic stem cells *in vitro* and in a xenograft mouse model *in vivo*. *Cytotherapy* 2013;15:986-98.
55. Smith LJ, Ul-Hasan T, Carvaines SK, Van Vliet K, Yang E, Wong KK Jr, et al. Gene transfer properties and structural modeling of human stem cell-derived AAV. *Mol Ther* 2014;22:1625-34.
56. Wang J, Exline CM, DeClercq JJ, Llewellyn GN, Hayward SB, Li PW, et al. Homology-driven genome editing in hematopoietic stem and progenitor cells using ZFN mRNA and AAV6 donors. *Nat Biotech* 2015;33:1256-63.
57. Han Z, Zhong L, Maina N, Hu Z, Li X, Chouhain NS, et al. Stable integration of recombinant adeno-associated virus vector genomes after transduction of murine hematopoietic stem cells. *Hum Gene Ther* 2008;19:267-78.
58. Au-Yeung BB, Shah NH, Shen L, Weiss A. ZAP-70 in signaling, biology, and disease. *Annu Rev Immunol* 2018;36:127-56.
59. Lopes N, Vachon H, Marie J, Irla M. Administration of RANKL boosts thymic regeneration upon bone marrow transplantation. *EMBO Mol Med* 2017;9:835-51.
60. Gillet NA, Malani N, Melamed A, Gormley N, Carter R, Bentley D, et al. The host genomic environment of the provirus determines the abundance of HTLV-1-infected T-cell clones. *Blood* 2011;117:3113-22.
61. Firouzi S, Lopez Y, Suzuki Y, Nakai K, Sugano S, Yamochi T, et al. Development and validation of a new high-throughput method to investigate the clonality of HTLV-1-infected cells based on provirus integration sites. *Genome Med* 2014;6:46.
62. Martin AT, Herzog RW, Anegón I, Adjali O. Measuring immune responses to recombinant AAV gene transfer. *Methods Mol Biol* 2011;807:259-72.
63. Li QZ, Zhou J, Wandstrat AE, Carr-Johnson F, Branch V, Karp DR, et al. Protein array autoantibody profiles for insights into systemic lupus erythematosus and incomplete lupus syndromes. *Clin Exp Immunol* 2007;147:60-70.
64. Capo V, Castiello MC, Fontana E, Penna S, Bosticardo M, Draghici E, et al. Efficacy of lentivirus-mediated gene therapy in an Omenn syndrome recombination-activating gene 2 mouse model is not hindered by inflammation and immune dysregulation. *J Allergy Clin Immunol* 2018;142:928-41.e8.
65. Rucci F, Poliani PL, Caraffi S, Paganini T, Fontana E, Giliani S, et al. Abnormalities of thymic stroma may contribute to immune dysregulation in murine models of leaky severe combined immunodeficiency. *Front Immunol* 2011;2.
66. Abramson J, Anderson G. Thymic Epithelial Cells. *Annu Rev Immunol* 2017;35:85-118.
67. Anderson MS, Venanzio ES, Klein L, Chen Z, Berzins SP, Turley SJ, et al. Projection of an immunological self shadow within the thymus by the Aire protein. *Science* 2002;298:1395-401.
68. Lopes N, Serge A, Ferrier P, Irla M. Thymic crosstalk coordinates medulla organization and T-cell tolerance induction. *Front Immunol* 2015;6:365.
69. Abramson J, Goldfarb Y. AIRE: from promiscuous molecular partnerships to promiscuous gene expression. *Eur J Immunol* 2016;46:22-33.
70. Irla M, Guerri L, Guenot J, Serge A, Lantz O, Liston A, et al. Antigen recognition by autoreactive CD4(+) thymocytes drives homeostasis of the thymic medulla. *PLoS One* 2012;7:e52591.
71. Gabler J, Arnold J, Kyewski B. Promiscuous gene expression and the developmental dynamics of medullary thymic epithelial cells. *Eur J Immunol* 2007;37:3363-72.
72. Gray D, Abramson J, Benoist C, Mathis D. Proliferative arrest and rapid turnover of thymic epithelial cells expressing Aire. *J Exp Med* 2007;204:2521-8.
73. Spangrude GJ, Scollay R. Differentiation of hematopoietic stem cells in irradiated mouse thymic lobes. Kinetics and phenotype of progeny. *J Immunol* 1990;145:3661-8.
74. Love PE, Bhandoola A. Signal integration and crosstalk during thymocyte migration and emigration. *Nat Rev Immunol* 2011;11:469-77.
75. McCaughtry TM, Wilken MS, Hogquist KA. Thymic emigration revisited. *J Exp Med* 2007;204:2513-20.
76. Kimura MY, Thomas J, Tai X, Guinter TI, Shinzawa M, Etzensperger R, et al. Timing and duration of MHC I positive selection signals are adjusted in the thymus to prevent lineage errors. *Nat Immunol* 2016;17:1415-23.
77. Thomas-Vaslin V, Altes HK, de Boer RJ, Klatzmann D. Comprehensive assessment and mathematical modeling of T cell population dynamics and homeostasis. *J Immunol* 2008;180:2240-50.
78. Perera J, Huang H. The development and function of thymic B cells. *Cell Mol Life Sci* 2015;72:2657-63.
79. Perera J, Meng L, Meng F, Huang H. Autoreactive thymic B cells are efficient antigen-presenting cells of cognate self-antigens for T cell negative selection. *Proc Natl Acad Sci U S A* 2013;110:17011-6.
80. Kumar SR, Markusic DM, Biswas M, High KA, Herzog RW. Clinical development of gene therapy: results and lessons from recent successes. *Mol Ther Methods Clin Dev* 2016;3:16034.
81. Colella P, Ronzitti G, Mingozzi F. Emerging issues in AAV-mediated *in vivo* gene therapy. *Mol Ther Methods Clin Dev* 2018;8:87-104.
82. Liu X, Adams A, Wildt KF, Aronow B, Feigenbaum L, Bosselut R. Restricting Zap70 expression to CD4+CD8+ thymocytes reveals a T cell receptor-dependent proofreading mechanism controlling the completion of positive selection. *J Exp Med* 2003;197:363-73.

83. Gascoigne NR, Palmer E. Signaling in thymic selection. *Curr Opin Immunol* 2011;23:207-12.
84. Singer A, Adoro S, Park JH. Lineage fate and intense debate: myths, models and mechanisms of CD4- versus CD8-lineage choice. *Nat Rev Immunol* 2008;8:788-801.
85. Etzensperger R, Kadakia T, Tai X, Alag A, Guinter TI, Egawa T, et al. Identification of lineage-specifying cytokines that signal all CD8(+)cytotoxic-lineage-fate 'decisions' in the thymus. *Nat Immunol* 2017;18:1218-27.
86. Nowrouzi A, Penaud-Budloo M, Kaeppel C, Appelt U, Le Guiner C, Moullier P, et al. Integration frequency and intermolecular recombination of rAAV vectors in non-human primate skeletal muscle and liver. *Mol Ther* 2012;20:1177-86.
87. Davis MM, Bjorkman PJ. T-cell antigen receptor genes and T-cell recognition. *Nature* 1988;334:395-402.
88. Wang CY, Yu PF, He XB, Fang YX, Cheng WY, Jing ZZ.  $\alpha\beta$  T-cell receptor bias in disease and therapy (review). *Int J Oncol* 2016;48:2247-56.
89. Calcedo R, Somanathan S, Qin Q, Betts MR, Rech AJ, Vonderheide RH, et al. Class I-restricted T-cell responses to a polymorphic peptide in a gene therapy clinical trial for alpha-1-antitrypsin deficiency. *Proc Natl Acad Sci U S A* 2017;114:1655-9.
90. Mingozzi F, High KA. Immune responses to AAV vectors: overcoming barriers to successful gene therapy. *Blood* 2013;122:23-36.
91. Xiao W, Chirmule N, Schnell MA, Tazelaar J, Hughes JV, Wilson JM. Route of administration determines induction of T-cell-independent humoral responses to adeno-associated virus vectors. *Mol Ther* 2000;1:323-9.
92. Mendoza SD, El-Shamayleh Y, Horwitz GD. AAV-mediated delivery of optogenetic constructs to the macaque brain triggers humoral immune responses. *J Neurophysiol* 2017;117:2004-13.
93. Walter JE, Rosen LB, Csomos K, Rosenberg JM, Mathew D, Keszei M, et al. Broad-spectrum antibodies against self-antigens and cytokines in RAG deficiency. *J Clin Invest* 2016;126:4389.
94. Surh CD, Sprent J. Regulation of mature T cell homeostasis. *Semin Immunol* 2005;17:183-91.
95. Cowan JE, Parnell SM, Nakamura K, Caamano JH, Lane PJ, Jenkinson EJ, et al. The thymic medulla is required for Foxp3<sup>+</sup> regulatory but not conventional CD4<sup>+</sup> thymocyte development. *J Exp Med* 2013;210:675-81.
96. van Ewijk W, Wang B, Hollander G, Kawamoto H, Spanopoulou E, Itoi M, et al. Thymic microenvironments, 3-D versus 2-D? *Semin Immunol* 1999;11:57-64.
97. Su DM, Navarre S, Oh WJ, Condie BG, Manley NR. A domain of Foxn1 required for crosstalk-dependent thymic epithelial cell differentiation. *Nat Immunol* 2003;4:1128-35.
98. Dudakov JA, van den Brink MR. Greater than the sum of their parts: combination strategies for immune regeneration following allogeneic hematopoietic stem cell transplantation. *Best Pract Res Clin Haematol* 2011;24:467-76.
99. Sutherland JS, Goldberg GL, Hammett MV, Uldrich AP, Berzins SP, Heng TS, et al. Activation of thymic regeneration in mice and humans following androgen blockade. *J Immunol* 2005;175:2741-53.
100. Goldberg GL, Dudakov JA, Reiseger JJ, Seach N, Ueno T, Vlahos K, et al. Sex steroid ablation enhances immune reconstitution following cytotoxic antineoplastic therapy in young mice. *J Immunol* 2010;184:6014-24.
101. Velardi E, Tsai JJ, Holland AM, Wertheimer T, Yu VW, Zakrzewski JL, et al. Sex steroid blockade enhances thymopoiesis by modulating Notch signaling. *J Exp Med* 2014;211:2341-9.
102. Min D, Panoskaltsis-Mortari A, Kuro OM, Hollander GA, Blazar BR, Weinberg KI. Sustained thymopoiesis and improvement in functional immunity induced by exogenous KGF administration in murine models of aging. *Blood* 2007;109:2529-37.
103. Rossi SW, Jeker LT, Ueno T, Kuse S, Keller MP, Zuklys S, et al. Keratinocyte growth factor (KGF) enhances postnatal T-cell development via enhancements in proliferation and function of thymic epithelial cells. *Blood* 2007;109:3803-11.
104. Dudakov JA, Hanash AM, Jenq RR, Young LF, Ghosh A, Singer NV, et al. Interleukin-22 drives endogenous thymic regeneration in mice. *Science* 2012;336:91-5.
105. Reimann C, Six E, Dal-Cortivo L, Schiavo A, Appourchaux K, Lagresle-Peyrou C, et al. Human T-lymphoid progenitors generated in a feeder-cell-free Delta-like-4 culture system promote T-cell reconstitution in NOD/SCID/gammac(-/-) mice. *Stem Cells* 2012;30:1771-80.
106. Awong G, Singh J, Mohatahami M, Malm M, La Motte-Mohs RN, Benveniste PM, et al. Human proT-cells generated in vitro facilitate hematopoietic stem cell-derived T-lymphopoiesis in vivo and restore thymic architecture. *Blood* 2013;122:4210-9.
107. Dudakov JA, Mertelsmann AM, O'Connor MH, Jenq RR, Velardi E, Young LF, et al. Loss of thymic innate lymphoid cells leads to impaired thymopoiesis in experimental graft-versus-host disease. *Blood* 2017;130:933-42.
108. Kelly RM, Goren EM, Taylor PA, Mueller SN, Stefanski HE, Osborn MJ, et al. Short-term inhibition of p53 combined with keratinocyte growth factor improves thymic epithelial cell recovery and enhances T-cell reconstitution after murine bone marrow transplantation. *Blood* 2010;115:1088-97.
109. Manna S, Bhandoola A. Intrathymic Injection. *Methods Mol Biol* 2016;1323:203-9.
110. Maina N, Han Z, Li X, Hu Z, Zhong L, Bischof D, et al. Recombinant self-complementary adeno-associated virus serotype vector-mediated hematopoietic stem cell transduction and lineage-restricted, long-term transgene expression in a murine serial bone marrow transplantation model. *Hum Gene Ther* 2008;19:376-83.
111. Ling C, Bhukhai K, Yin Z, Tan M, Yoder MC, Leboulch P, et al. High-efficiency transduction of primary human hematopoietic stem/progenitor cells by AAV6 vectors: strategies for overcoming donor-variation and implications in genome editing. *Sci Rep* 2016;6:35495.
112. Huser D, Khalid D, Lutter T, Hammer EM, Weger S, Hessler M, et al. High prevalence of infectious adeno-associated virus (AAV) in human peripheral blood mononuclear cells indicative of T lymphocytes as sites of AAV persistence. *J Virol* 2017;91.
113. Vandamme C, Adjali O, Mingozzi F. Unraveling the complex story of immune responses to AAV vectors trial after trial. *Hum Gene Ther* 2017;28:1061-74.
114. Reichel FF, Peters T, Wilhelm B, Biel M, Ueffing M, Wissinger B, et al. Humoral immune response after intravitreal but not after subretinal AAV8 in primates and patients. *Invest Ophthalmol Vis Sci* 2018;59:1910-5.
115. Reichel FF, Dauletbekov DL, Klein R, Peters T, Ochakovski GA, Seitz IP, et al. AAV8 can induce innate and adaptive immune response in the primate eye. *Mol Ther* 2017;25:2648-60.
116. McIntosh JH, Cochrane M, Cobbold S, Waldmann H, Nathwani SA, Davidoff AM, et al. Successful attenuation of humoral immunity to viral capsid and transgenic protein following AAV-mediated gene transfer with a non-depleting CD4 antibody and cyclosporine. *Gene Ther* 2012;19:78-85.
117. Han SO, Li S, Brooks ED, Masat E, Leborgne C, Banugaria S, et al. Enhanced efficacy from gene therapy in Pompe disease using coreceptor blockade. *Hum Gene Ther* 2015;26:26-35.
118. Corti M, Elder M, Falk D, Lawson L, Smith B, Nayak S, et al. B-cell depletion is protective against anti-AAV capsid immune response: a human subject case study. *Mol Ther Methods Clin Dev* 2014;1.
119. Mack DL, Poulard K, Goddard MA, Latournerie V, Snyder JM, Grange RW, et al. Systemic AAV8-mediated gene therapy drives whole-body correction of myotubular myopathy in dogs. *Mol Ther* 2017;25:839-54.
120. Elverman M, Goddard MA, Mack D, Snyder JM, Lawlor MW, Meng H, et al. Long-term effects of systemic gene therapy in a canine model of myotubular myopathy. *Muscle Nerve* 2017;56:943-53.
121. Le Guiner C, Servais L, Montus M, Larcher T, Fraysse B, Moullec S, et al. Long-term microdystrophin gene therapy is effective in a canine model of Duchenne muscular dystrophy. *Nat Commun* 2017;8:16105.
122. Mueller C, Chulay JD, Trapnell BC, Humphries M, Carey B, Sandhaus RA, et al. Human Treg responses allow sustained recombinant adeno-associated virus-mediated transgene expression. *J Clin Invest* 2013;123:5310-8.
123. Germoux G, Wilson JM, Mueller C. Regulatory and exhausted T cell responses to AAV capsid. *Hum Gene Ther* 2017;28:338-49.
124. Foss DL, Donskoy E, Goldschneider I. The importation of hematogenous precursors by the thymus is a gated phenomenon in normal adult mice. *J Exp Med* 2001;193:365-74.
125. Prockop SE, Petrie HT. Regulation of thymus size by competition for stromal niches among early T cell progenitors. *J Immunol* 2004;173:1604-11.
126. Adjali O, Vicente RR, Ferrand C, Jacquet C, Mongellaz C, Tiberghien P, et al. Intrathymic administration of hematopoietic progenitor cells enhances T cell reconstitution in ZAP-70 severe combined immunodeficiency. *Proc Natl Acad Sci U S A* 2005;102:13586-91.
127. de Barros SC, Vicente R, Chebli K, Jacquet C, Zimmermann VS, Taylor N. Intrathymic progenitor cell transplantation across histocompatibility barriers results in the persistence of early thymic progenitors and T-cell differentiation. *Blood* 2013;121:2144-53.
128. Hirschhorn R, Yang DR, Puck JM, Huie ML, Jiang CK, Kurlandsky LE. Spontaneous in vivo reversion to normal of an inherited mutation in a patient with adenosine deaminase deficiency. *Nat Genet* 1996;13:290-5.
129. Bousso P, Wahn V, Douagi I, Horneff G, Pannetier C, Le Deist F, et al. Diversity, functionality, and stability of the T cell repertoire derived in vivo from a single human T cell precursor. *Proc Natl Acad Sci U S A* 2000;97:274-8.
130. Stephan V, Wahn V, Le Deist F, Dirksen U, Broker B, Muller-Fleckenstein I, et al. Atypical X-linked severe combined immunodeficiency due to possible spontaneous reversion of the genetic defect in T cells. *N Engl J Med* 1996;335:1563-7.

131. Ariga T, Oda N, Yamaguchi K, Kawamura N, Kikuta H, Taniuchi S, et al. T-cell lines from 2 patients with adenosine deaminase (ADA) deficiency showed the restoration of ADA activity resulted from the reversion of an inherited mutation. *Blood* 2001;97:2896-9.
132. Wada T, Konno A, Schurman SH, Garabedian EK, Anderson SM, Kirby M, et al. Second-site mutation in the Wiskott-Aldrich syndrome (WAS) protein gene causes somatic mosaicism in two WAS siblings. *J Clin Invest* 2003;111:1389-97.
133. Davis BR, Yan Q, Bui JH, Felix K, Moratto D, Muul LM, et al. Somatic mosaicism in the Wiskott-Aldrich syndrome: molecular and functional characterization of genotypic revertants. *Clin Immunol* 2010;135:72-83.
134. Davis BR, Dicola MJ, Prokopishyn NL, Rosenberg JB, Moratto D, Muul LM, et al. Unprecedented diversity of genotypic revertants in lymphocytes of a patient with Wiskott-Aldrich syndrome. *Blood* 2008;111:5064-7.
135. Rieux-Lauca F, Hivroz C, Lim A, Mateo V, Pellier I, Selz F, et al. Inherited and somatic CD3 $\zeta$  mutations in a patient with T-cell deficiency. *N Engl J Med* 2006;354:1913-21.
136. Wada T, Toma T, Okamoto H, Kasahara Y, Koizumi S, Agematsu K, et al. Oligoclonal expansion of T lymphocytes with multiple second-site mutations leads to Omenn syndrome in a patient with RAG1-deficient severe combined immunodeficiency. *Blood* 2005;106:2099-101.
137. Tone Y, Wada T, Shibata F, Toma T, Hashida Y, Kasahara Y, et al. Somatic revertant mosaicism in a patient with leukocyte adhesion deficiency type 1. *Blood* 2007;109:1182-4.
138. Nishikomori R, Akutagawa H, Maruyama K, Nakata-Hizume M, Ohmori K, Mizuno K, et al. X-linked ectodermal dysplasia and immunodeficiency caused by reversion mosaicism of NEMO reveals a critical role for NEMO in human T-cell development and/or survival. *Blood* 2004;103:4565-72.
139. Uzel G, Tng E, Rosenzweig SD, Hsu AP, Shaw JM, Horwitz ME, et al. Reversion mutations in patients with leukocyte adhesion deficiency type-1 (LAD-1). *Blood* 2008;111:209-18.
140. Speckmann C, Pannicke U, Wiech E, Schwarz K, Fisch P, Friedrich W, et al. Clinical and immunologic consequences of a somatic reversion in a patient with X-linked severe combined immunodeficiency. *Blood* 2008;112:4090-7.

## METHODS

### AAV constructs and vector production

The human ZAP70 gene was cloned downstream of the murine phosphoglycerate kinase promoter with the bovine growth hormone (BGH) polyadenylation signal sequences flanked by 2 AAV2-ITR sequences. For the GFP coding vector plasmid, the phosphoglycerate kinase promoter is upstream of the GFP sequence and the simian virus 40 polyadenylation signal.

Self-complementary adeno-associated virus (scAAV) 8, scAAV9, and scAAV10 harboring GFP and single-stranded AAV-8 harboring ZAP-70 vector stocks were produced by means of cotransfection of HEK 293 cells with the vector plasmid and the pDG plasmid,<sup>E1</sup> an adenoviral plasmid providing helper functions needed for rAAV assembly, as previously described.<sup>E2</sup> Supernatants were precipitated with polyethylene glycol (Sigma-Aldrich, St Louis, Mo) and resuspended in Tris-buffered saline before benzonase digestion. Vector-containing supernatants were purified on a double CsCl gradient, with the first gradient centrifuged at 28,000 rpm for 24 hours at 15°C, and the band harboring full particles was centrifuged at 38,000 rpm for 48 hours. Viral suspensions were then subjected to 4 successive rounds of dialysis against Dulbecco-PBS in a Slide-A-Lyzer Cassette (Thermo Scientific, Waltham, Mass). The number of infectious particles per milliliter in the purified vector preparation was determined by using a stable rep/cap HeLa cell line in a modified replication center assay.<sup>E3</sup> Vectors were stored at less than -70°C in polypropylene low-binding cryovials.

### Mice and intrathymic AAV gene therapy

C57Bl/6 and ZAP-70<sup>-/-</sup> mice were maintained under specific pathogen-free conditions in the IGMM animal facility (Montpellier, France). Serum from female MRL/lpr and sex-matched control MRL/MpJ mice were generously provided by Luz Blanco and Mariana Kaplan (National Institute of Arthritis and Musculoskeletal and Skin Diseases/National Institutes of Health). Intrathymic injections were performed in 2.5- to 3-week-old nonconditioned mice with rAAV vectors (1-3 × 10<sup>13</sup> vector genomes/kg), as previously described.<sup>E4</sup> Briefly, nonconditioned mice were anesthetized with isoflurane, and vectors were directly injected into the thymus (20 μL of total volume) through insertion of a 0.3-mL, 28-gauge, 8-mm insulin syringe through the skin into the thoracic cavity above the sternum. All experiments were approved by the local animal facility institutional review board in accordance with national guidelines.

### Immunophenotyping, T-cell activation, and flow cytometric analyses

Cells isolated from the thymi, lymph nodes, or spleen were stained with the appropriate conjugated αCD3, αCD4, αCD8, αCD11b, αCD19, αCD25, αCD62L, αCD39, αCD44 αCTLA4, and αGITR mAbs (Becton Dickinson, San Diego, Calif). Intracellular staining for FOXP3 and ZAP-70 was performed after fixation/permeabilization (eBioscience, San Diego, Calif) and the BD Biosciences (San Jose, Calif) kit, respectively. Cell activation was performed with plate-bound anti-CD3 (clone 17A2, 1 μg/mL) and anti-CD28 (clone PV-1, 1 μg/mL) mAbs in RPMI 1640 media (Life Technologies, Grand Island, NY) supplemented with 10% FCS. Cell proliferation was monitored by labeling with CellTrace Violet (5 μmol/L; Life Technologies) for 3 minutes at room temperature. Cytokine production was monitored with a Cytometric Bead Array Kit (BD Biosciences). Stained cells were analyzed by using flow cytometry (FACSCanto II or LSR II Fortessa; Becton Dickinson, San Jose, Calif). Data analyses were performed with FACSDiva (BD Biosciences), FlowJo Mac (version 10.4.2; TreeStar, Ashland, Ore), and FCAP Array (BD Biosciences) software.

### Immunohistochemistry

Frozen thymic sections were stained, as previously described.<sup>E5</sup> Sections were stained with anti-keratin 14 (1:800; AF64; Covance, Princeton, NJ) and a secondary Cy3-conjugated anti-rabbit (1:500; Invitrogen, Carlsbad, Calif) antibody together with an Alexa Fluor 488-conjugated anti-AIRE

mAb (1:200; 5H12; eBioscience). They were then counterstained with 1 μg/mL 4'-6-diamidino-2-phenylindole dihydrochloride, as previously reported.<sup>E6</sup> Images were acquired on LSM 780 (Zeiss, Oberkochen, Germany) and SP5 (Leica, Wetzlar, Germany) confocal microscopes and quantified with ImageJ (National Institutes of Health) and MATLAB software.

### Quantitative real-time PCR for evaluation of vector genomes and quantitative RT-PCR for cellular genes

Total DNA was extracted with the Gentra Puregene Kit (Qiagen, Hilden, Germany) and TissueLyser II (Qiagen), according to the manufacturer's instructions. Vector genome DNA was measured through quantification of *Bgh-pA* by using quantitative PCR (qPCR) with the Premix Ex Taq kit (TAKARA BIO, Kusatsu, Japan). Primers were as follows: 5'-TCTAGTTGC CAGCCATCTGTTGT-3' (forward) and 5'-TGGGAGTGGCACCTTCCA-3' (reverse). The *Bgh-pA* TaqMan probe was as follows: 5'-(6 FAM)-TCCCCCGTCCTCCTTGACC-(TAMRA)-3'. Primers for endogenous albumin were as follows: 5'-ACATAGCTTGCCTCAGAACGGT-3' (forward) and 5'-AGTGTCTTCATCCTGCCCTAAA-3' (reverse). qPCR for *Bgh-pA* was performed with the following program: initial denaturation for 20 seconds at 95°C, followed by 45 cycles of 1 second at 95°C and 20 seconds at 60°C. qPCR for albumin was performed as follows: initial denaturation for 20 seconds at 95°C, followed by 45 cycles of 3 seconds at 90°C and 30 seconds at 60°C. For each qPCR, cycle threshold values were compared with those obtained by using dilutions of plasmids harboring either the *Bgh-pA* or albumin genes, and results are expressed as vector genomes per diploid genome.

For assessment of *I10* and *Foxp3* mRNA levels, CD4<sup>+</sup>CD25<sup>-</sup> and CD4<sup>+</sup>CD25<sup>hi</sup> cells from WT and intrathymic AAV8-ZAP-70 mice (15 weeks after injection) were sorted on a FACSaria, and RNA extraction was performed with the RNeasy Mini kit (Qiagen). RNA was reverse transcribed into cDNA by means of oligonucleotide priming with the QuantiTect Reverse Transcription Kit (Qiagen). Each sample was amplified in triplicates (LightCycler 480; Roche, Mannheim, Germany) and normalized to hypoxanthine phosphoribosyltransferase (*Hprt*) levels using the following specific primers: *Foxp3* sense, 5'-GGCCCTTCTCCAGGACAGA-3'; *Foxp3* antisense, 5'-GCTGATCATGGCTGGTTGT-3'; *I10* sense, 5'-AACTGCT CCACTGCCTTGCT-3'; *I10* antisense, 5'-GTTGCCAAGCCTATC GGA-3'; *Hprt* sense, 5'-CTGGTGAA-AAGGACCTCTCG-3'; and *Hprt* antisense, 5'-TGAAGTACTCATTATACTCAAGGGCA-3'.

### Vector integration analysis

To assess AAV integration, we adopted a sonication-based linker-mediated PCR method, as previously described.<sup>E7,E8</sup> Briefly, genomic DNA was sheared with a Covaris E220 Ultrasonicator, generating fragments with a target size of 1000 bp. The fragmented DNA was subjected to end repair, 3' adenylation, and ligation (NEBNext Ultra DNA Library Prep Kit for Illumina [New England Biolabs, Ipswich, Mass]) to custom LCs (Integrated DNA Technologies, Coralville, Iowa). LC sequences contain (1) an 8-nucleotide barcode used for sample identification and (2) 12 random nucleotides used for quantification purposes. Ligation products were subjected to 35 cycles of exponential PCR with primers complementary to 8 different regions of the AAV genome (see Fig 4, C, and primers available on request) and the LC. For each set of AAV-specific primers, the procedure was performed in technical replicates (n = 2-3) starting from 5 to 120 ng of sheared DNA.

All final PCR products were quantified by using qPCR with the Kapa Biosystems Library Quantification Kit for Illumina (San Diego, Calif), according to the manufacturer's instructions. qPCR was performed in triplicate on each PCR product diluted 10<sup>-3</sup>, and concentrations were calculated by plotting average cycle threshold values against the provided standard curve using absolute quantification.

### TCR deep sequencing and data processing

Cells from lymph nodes were pooled and lysed, and RNAs were extracted. TCRα/β libraries were prepared with 100 ng of total RNA from each sample by using the SMARTer Mouse TCRα/β Profiling Kit from TAKARA BIO and

sequenced by using the MiSeq V3 2 × 300bp (Illumina). Raw data were aligned and curated with the MiXCR software (version 2.1.10).<sup>E9</sup> The α and β chains were analyzed together. Each sample was defined as a combination of *Trv-cdr3aa-Trj* sequences and their associated counts.

For representation and analyses, data sets were normalized by a sampling step. The sampling size was equal to the smallest sequence number observed in the analyzed samples (n = 687). Sampling was performed for each data set by 100 random draws of sequences, and unique TCRs were listed and counted. Analyses and figures were executed and created with R Studio software (v3.5.0).

## Evaluation of humoral immune responses

For evaluation of *in vivo* T-cell responses, WT and AAV8-reconstituted mice (46 weeks after gene transfer, 49 weeks of age) were immunized with OVA (3 × 200 µg complexed with complete Freund adjuvant at day 0, incomplete Freund adjuvant at day 14, and LPS at day 28). Serum IgG levels were evaluated at time 0 and 6 weeks after immunization by using an ELISA. Serum anti-ZAP-70 antibodies were evaluated by means of ELISA at different time points after gene transfer. Briefly, 96-well plates (Nunc MaxiSorp, Thermo Scientific) were coated with recombinant ZAP-70 protein (0.5 µg/mL; Thermo Scientific), sera were added at 1:100 and 1:500 dilutions, and a standard scale was generated by serial dilutions of an anti-ZAP-70 mAb (clone 1E7.2; Thermo Scientific). Responsiveness was monitored by using horseradish peroxidase-conjugated goat anti-mouse IgG (Dako, Glostrup, Denmark) and revealed with 2,2'-3,3',5,5'-tetramethylbenzidine (BD OptEIA; BD Biosciences). The threshold of positivity was determined by averaging the signal of 23 negative sera obtained from naive or AAV GFP-injected mice ± 2\*SD. Serum anti-dsDNA, anti-RNP, and anti-SSA levels were quantified by means of ELISA according to the manufacturer's instructions (Alpha Diagnostic International, San Antonio, Tex).

The presence of neutralizing antibody in serum samples was monitored, as previously described.<sup>E10</sup> Two hours before rAAV infection, a permissive cell line was infected with WT adenovirus, serotype 5. During this incubation time, a rAAV2/rAAV8 expressing the reporter gene *LacZ* (encoding β-galactosidase) was incubated with serial dilutions of serum, and the mix was added to the cell line. Infection was assessed by using the luminescent β-galactosidase substrate (Tropix Galacto-Star Kit; Thermo Scientific) at 48 hours. The neutralizing capacity of a given serum is expressed as the titer corresponding to the greatest serum dilution at which more than 50% of maximal infection is inhibited.

Screening for IgM and IgG reactivity against 123 autoantigens was performed by using autoantibody arrays (UT Southwestern Medical Center, Genomic and Microarray Core Facility, Dallas, Tex), as previously described,<sup>E11,E12</sup> and heat maps were generated with R software.

## Statistical analyses

Data were analyzed with GraphPad Prism software (version 5 and 8; GraphPad Software, La Jolla, Calif), and P values were calculated by using unpaired *t* tests, 1-way ANOVA (Tukey multiple comparison test), and Mann-Whitney tests, as indicated. P values for comparisons of all conditions in the different figure panels are presented in the figure legends.

## REFERENCES

- E1. Grimm D, Kay MA, Kleinschmidt JA. Helper virus-free, optically controllable, and two-plasmid-based production of adeno-associated virus vectors of serotypes 1 to 6. *Mol Ther* 2003;7:839-50.
- E2. Chenuaud P, Larcher T, Rabinowitz JE, Provost N, Jousset B, Bujard H, et al. Optimal design of a single recombinant adeno-associated virus derived from serotypes 1 and 2 to achieve more tightly regulated transgene expression from nonhuman primate muscle. *Mol Ther* 2004;9:410-8.
- E3. Salvetti A, Oreve S, Chadeuf G, Favre D, Cherel Y, Champion-Arnaud P, et al. Factors influencing recombinant adeno-associated virus production. *Hum Gene Ther* 1998;9:695-706.
- E4. Vicente R, Adjali O, Jacquet C, Zimmermann VS, Taylor N. Intrathymic transplantation of bone marrow-derived progenitors provides long-term thymopoiesis. *Blood* 2010;115:1913-20.
- E5. Lopes N, Vachon H, Marie J, Irla M. Administration of RANKL boosts thymic regeneration upon bone marrow transplantation. *EMBO Mol Med* 2017;9: 835-51.
- E6. Serge A, Bailly AL, Aurrand-Lions M, Imhof BA, Irla M. For3D: full organ reconstruction in 3D, an automatized tool for deciphering the complexity of lymphoid organs. *J Immunol Methods* 2015;424:32-42.
- E7. Firouzi S, Lopez Y, Suzuki Y, Nakai K, Sugano S, Yamochi T, et al. Development and validation of a new high-throughput method to investigate the clonality of HTLV-1-infected cells based on provirus integration sites. *Genome Med* 2014;6:46.
- E8. Gillet NA, Malani N, Melamed A, Gormley N, Carter R, Bentley D, et al. The host genomic environment of the provirus determines the abundance of HTLV-1-infected T-cell clones. *Blood* 2011;117:3113-22.
- E9. Bolotin DA, Poslavsky S, Mitrophanov I, Shugay M, Mamedov IZ, Putintseva EV, et al. MiXCR: software for comprehensive adaptive immunity profiling. *Nat Methods* 2015;12:380-1.
- E10. Martino AT, Herzog RW, Anegón I, Adjali O. Measuring immune responses to recombinant AAV gene transfer. *Methods Mol Biol* 2011; 807:259-72.
- E11. Li QZ, Zhou J, Wandstrat AE, Carr-Johnson F, Branch V, Karp DR, et al. Protein array autoantibody profiles for insights into systemic lupus erythematosus and incomplete lupus syndromes. *Clin Exp Immunol* 2007; 147:60-70.
- E12. Capo V, Castiello MC, Fontana E, Penna S, Bosticardo M, Draghici E, et al. Efficacy of lentivirus-mediated gene therapy in an Omenn syndrome recombination-activating gene 2 mouse model is not hindered by inflammation and immune dysregulation. *J Allergy Clin Immunol* 2018;142:928-41.e8.

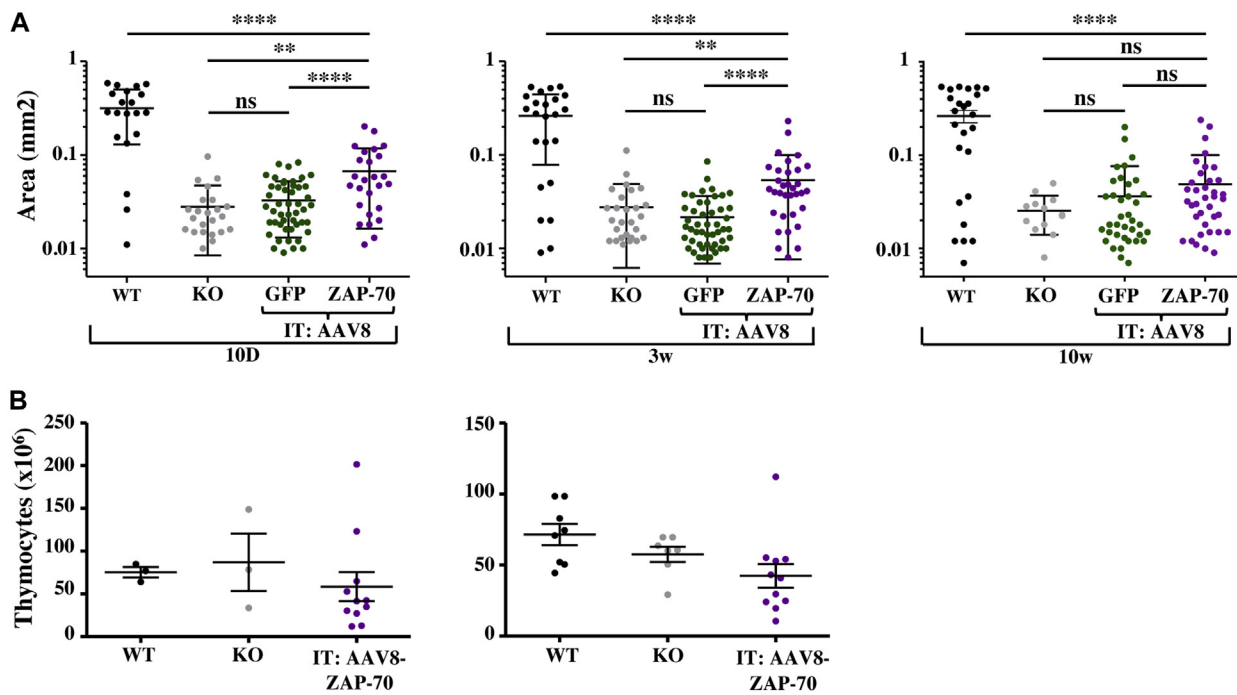


**FIG E1.** Intrathymic AAV8-ZAP-70 gene transfer results in alterations in the medullary area in  $ZAP-70^{-/-}$  mice. **A**, Thymic medullary area was evaluated based on keratin 14 (K14) staining. Representative confocal images of thymic tissue sections are presented in Fig 2. Quantification of the medullary area in square millimeters of thymus was quantified in the indicated conditions. Each point represents quantification of individual medullas derived from 2 to 3 mice at the indicated time points, and significance was determined by using a 2-tailed unpaired *t* test. ns, Not significant. \*\**P* < .01 and \*\*\*\**P* < .0001. **B**, Absolute numbers of thymocytes in intrathymic AAV8-ZAP-70-transduced KO mice (*n* = 11) were determined at 3 weeks after gene transfer, as well as in age-matched WT and KO control mice (*n* = 3–10). Each point represents an individual mouse, with horizontal lines showing means. Data between groups were not significantly different. *IT*, Intrathymic.

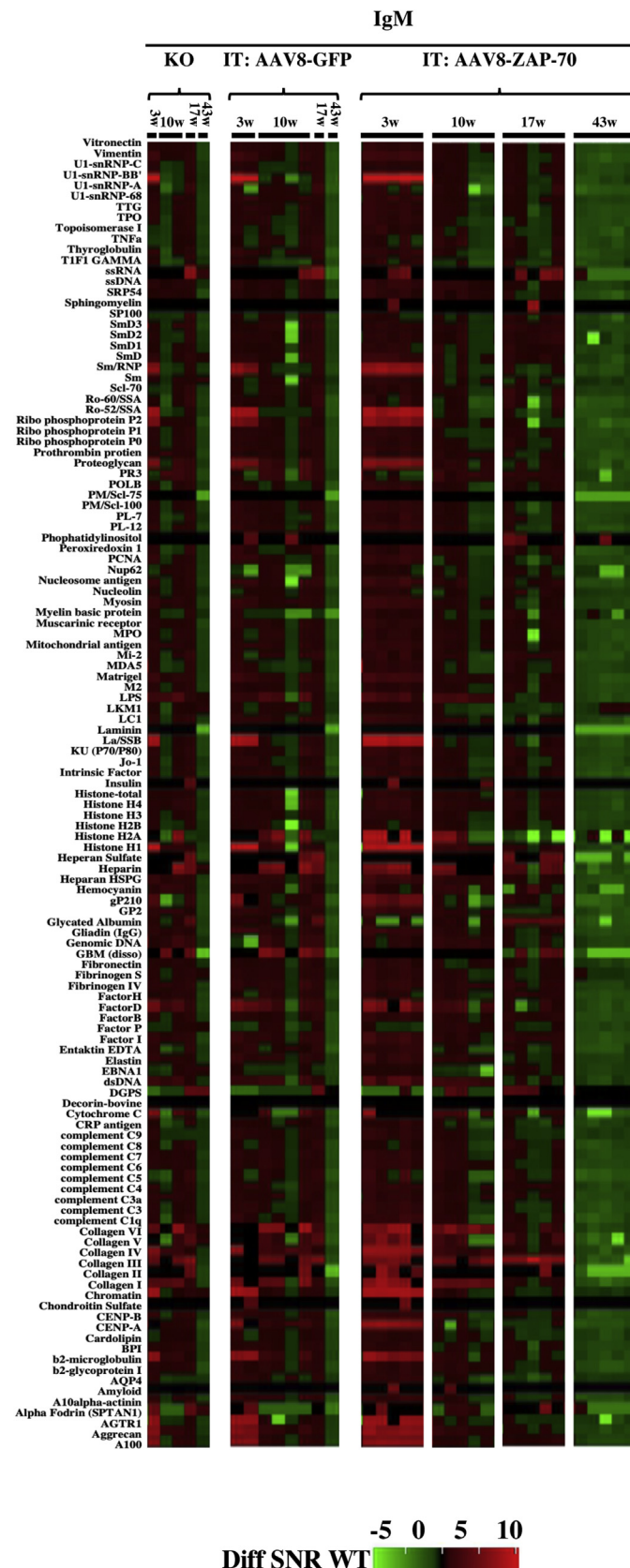


**FIG E2.** Transient induction of a broad spectrum of IgM antibodies in ZAP-70<sup>-/-</sup> mice after intrathymic AAV8 gene transfer. IgM autoantibody levels were evaluated in sera of ZAP-70<sup>-/-</sup> (KO) mice and after intrathymic administration of either AAV8-GFP or AAV8-ZAP-70 vectors at the indicated time points. IgM autoantibodies against 123 antigens were assessed by using a protein microarray. Heat maps showing autoantibody reactivity relative to levels in age-matched WT mice are presented. *IT*, Intrathymic; *SNR*, signal to noise ratio.

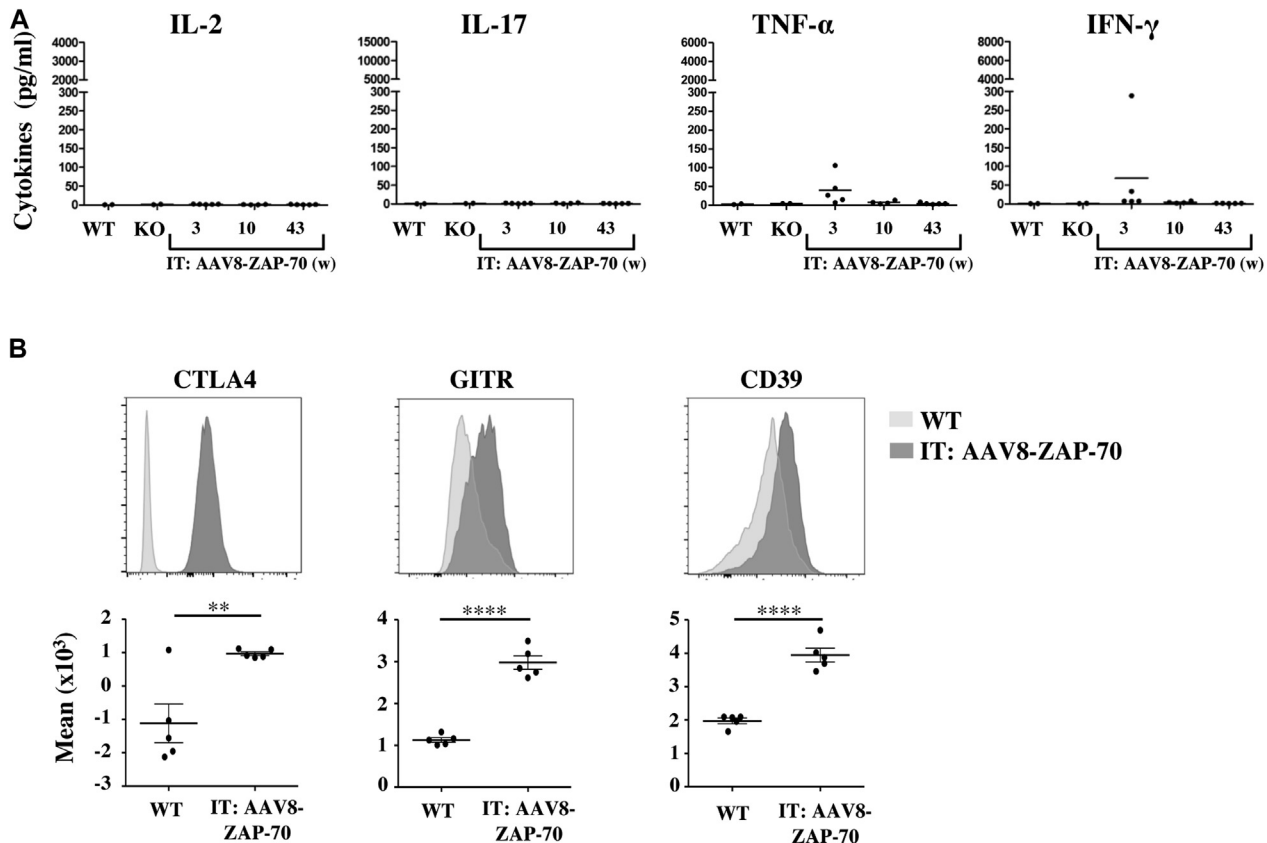


**FIG E3.** High expression of Treg cell markers in intrathymic AAV8-ZAP-70-transduced mice. **A**, Cytokine levels in sera of WT and ZAP-70<sup>-/-</sup> mice treated with intrathymic AAV8-ZAP-70 gene transfer was evaluated at 3, 10, and 43 weeks after injection by using a cytokine bead array. Each point represents data from a single mouse, and horizontal lines represent mean levels (in picograms per milliliter). Statistical significance was determined by using a 2-tailed Mann-Whitney test, and no groups exhibited significant differences. **B**, Surface levels of CTLA4, GITR, and CD39 on CD4<sup>+</sup>CD25<sup>hi</sup> T cells from WT and intrathymic AAV8-ZAP-70-transduced KO mice were evaluated by using flow cytometry, and representative histograms are shown (top). Quantification of mean fluorescence intensity in T cells from individual mice is presented, and significance was assessed by using an unpaired *t* test (bottom). \*\**P* < .01 and \*\*\*\**P* < .0001. *IT*, Intrathymic.